Source Rock Distributions and Petroleum Fluid Bulk Compositional Predictions on the Vulcan Sub-Basin, Offshore Western Australia

Volkmar Neumann
Rolando di Primio
Brian Horsfield

GeoS4 GmbH
Peter-Huchel-Chaussee 88
14552 Michendorf
Germany

Address: Telephone: Telefax: e-mail:	GeoS4 GmbH Peter-Huchel-Chaussee 88 14552 Michendorf Germany +49 3320523861 +49 3320523862 info@geos4.com
Report Number:	GeoS4 20081201
Report Title:	Source Rock Distributions and Petroleum Fluid Bulk Compositional Predictions on the Vulcan Sub-Basin, Offshore Western Australia
Author:	V. Neumann, R. di Primio, B Horsfield
Classification:	Confidential
Client:	Geoscience Australia
Client Reference:	
Distribution: Geoscience Australia GeoS4 GmbH	 1 + CD 1 + CD

V. Neumann | R. di Primio | B. Horsfield

Disclaimer

Introduction 5
Input Data 6
Data Base 6
Source Rocks 9
Seal Properties 14
Description of Modelling Scenarios 15
Simulation 16
Results 17
Scenario 1 21
Scenario 2 28
Scenario 3 34
Scenario 4 41
Scenario 5 46
Summary and Conclusions 50
References 55
Appendix 1 57
Compositional Kinetic Models 57
Cumulative Volumes 60
Appendix 2 62
Comparison of petroleum physical property predictions of 4-compound and PhaseKinetic models 62
Methodology and background information on the PhaseKinetics approach. 66

Introduction

The Vulcan Sub-basin is a northeast-southwest aligned Late Permian to Jurassic extensional depocenter in the western offshore Bonaparte Basin, located in the Timor Sea on the NW Australian margin, some 600 kilometres west of Darwin, within water depths of mostly less than 200 metres. Its major grabens are the Swan Graben and the Cartier Trough (Figure 1, Figure 3). The basin contains producing and decommissioned oil fields as well as currently undeveloped oil and gas discoveries. The organic rich Late Jurassic Vulcan Formation is the main hydrocarbon source rock of the Vulcan Sub-basin. The Plover Formation of Early to Middle Jurassic age can be seen as a secondary potential source. Based on earlier basin modelling results Geoscience Australia identified a need to predict the occurrence of petroleum, its composition as well as the distribution and type of organic matter in source kitchens in the Vulcan Sub-basin. This definition has to be in a form that can be directly translated into quantitative predictions of oil and gas volumes in time and space.

The Vulcan Sub-basin was subject of intensive basin modelling work, which was carried out using the PetroMod™ version 9 2D/3D basin modelling package. The software is based on a forward modeling approach to calculate the geologic evolution of a basin, starting at the oldest and finishing at the youngest event, using the present as key to the past (Yalcin et al., 1997). A detailed review of the IES basin modelling software and its concepts is given in the PetroMod™ reference manual (http://www.iesgmbh.eu). The results of the modelling were published by Fujii et al. (2004), and while their model calibration showed a very good match for the thermal regime, it fails to reproduce the composition and location of many hydrocarbons which have accumulated within the modelled area of the Vulcan Sub-Basin. This is basically a consequence of the kinetic data sets which have been used as well as the geographic distribution of the main source rock intervals within the basin. This cooperation between Geoscience Australia (GA) and GeoS4 GmbH (Germany) was initiated in order to conduct a regional investigation of 'Source Rock Distribution and Petroleum Fluid Bulk Compositional Predictions on the Vulcan-basin, offshore Western Australia'. This work forms an integral part of continuing studies by Geoscience Australia on the petroleum potential of the North-West shelf.

GA provided a thermally calibrated 3D basin model, which had been modelled with the basin modelling software suite PetroMod™ version 9 of IES Germany. This model was used for this study as a basis for testing a variety of scenarios on

- the geographic distribution of different source rock sequences
- the petrophysical properties of the assigned cap rocks
- the relative input of the individual source rock sequences on the total petroleum generated (oil families of Edward et al., 2004)

Furthermore, the supplied data set included

- an extensive report data base (general overview papers and special studies)
- calibration data (vitrinite reflectance, temperature, porosities) from several Vulcan Sub-basin wells
- Vulcan well composites

Numerical modelling for this report was performed using the basin modeling program PetroMod™ version 10, Patch 4 (IES, Germany).

Key References:

Fujii, T., O'Brien, G.W., Tingate, P.R., Chen, G., (2004) Using 2D and 3D basin modelling to investigate controls on hydrocarbon migration and accumulation in the Vulcan Sub-basin, Timor Sea, Northwestern Australia. APPEA Journal, 93-122.

Edwards, D.S., Preston, J.C., Kennard, J.M., Boreham, C.J., van Aarssen, B.G.K., Summons, R.E., Zumberge, J.E., (2004) Geochemical characteristics of hydrocarbons from the Vulcan Sub-basin, western Bonaparte Basin, Australia. Special Publication - Northern Territory Geological Survey, 1, 31.

Cadman, S.J., Temple, P.R., (2003) Bonaparte Basin, NT, WA, AC & JPDA. In: Australian Petroleum Accumulations Report 5, 2nd Edition, pp. 335. Geoscience Australia, Canberra.

Input Data

Data Base

127 exploration wells have been drilled in the greater Vulcan Sub-basin (Figure 1), resulting in 23 discoveries; six encountered oil, nine encountered gas, and eight encountered both oil and gas (Cadman & Temple, 2003). The majority of the exploration wells are located inside the digital area of the numerical model (Figure 3). 26 wells contain calibration data sets (temperature and vitrinite reflectance data) which were used in the previous studies for the thermal calibration of the model. Results obtained in this study were checked against the data sets in order to recognise variations in the quality of the thermal calibration, which might occur as a function of the new lithological definitions which were assigned to the sedimentary units in this study.

The original 3D model from Fujii et al. (2004), which is the basis for the modeling presented here, was constructed using a map stack of 11 interpreted and depth converted seismic surface maps. Their work was based on the interpretations of depth converted 2D seismic lines as published by Chen et al. (2002). The original numerical modelling by Fujii in 2002 was probably performed using the PetroMod version 8 (no reference is given), and then updated, first to version 9, then, in the present study, to version 10, which is the latest version.

The ASCII horizons and fault files were imported into the PetroMod™ software package.

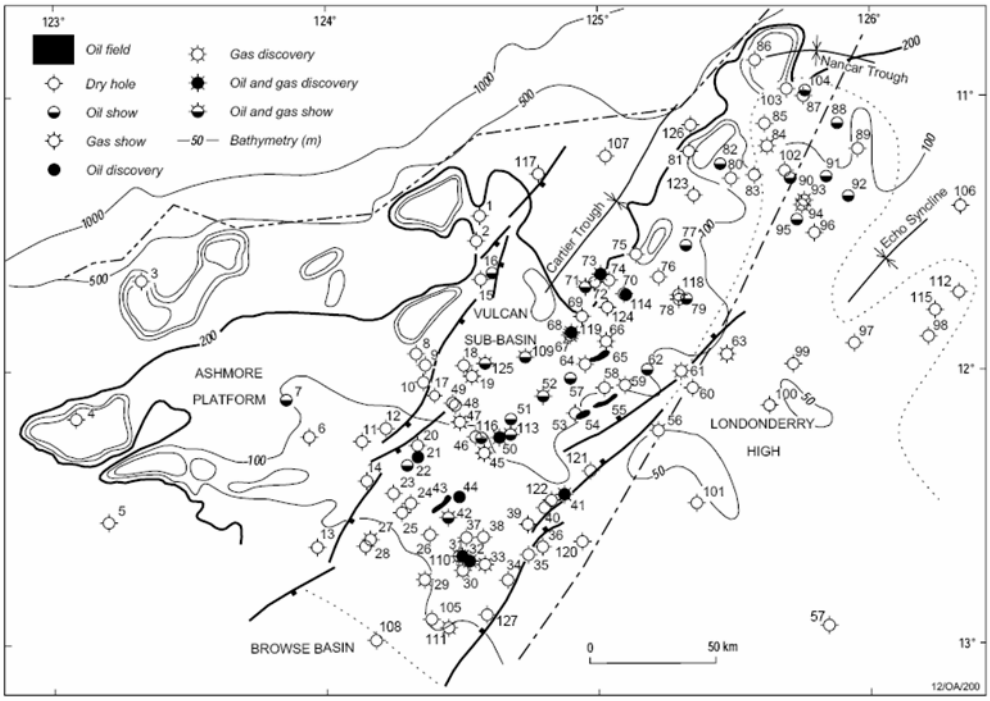

Figure 1 Major tectonic elements, bathymetry and exploration wells in the Vulcan Sub-basin and adjacent areas(Cadman & Temple, 2003).

In total, 15 sedimentary units were used for the definition of the numerical model. In agreement with GA, the original Plover Formation was subdivided into five individual sub-packages with the ratio of the original thickness as shown below.

- Plover_Sand: 10%
- Plover_SR: 9%
- Plover_Sand2: 60%
- Plover_Shale: 15 %
- Plover_Sand3: 6%

This subdivision is significantly different as compared to the original model of Fujii, who subdivided the Plover Formation into a sandy reservoir interval in the uppermost 20% of its thickness, and a shaly source rock interval for the rest. The subdivision was required as the presence of such a thick Plover source rock unit is not expected.

However, both the subdivision as well as the distribution of especially the source rock unit is highly speculative, as its distribution is only very poorly constrained by wells within the basin. For nearly all rock types of the original model PetroMod™ V.9 user-defined lithological definitions were assigned. The definitions available in PetroMod™ V.10 show recognisable variations as compared to the original definitions, in general the new lithological definitions are more permeable as compared to the V.9 definitions. From the point of view of migration and leakage the V.10 lithologies are better suited to reproduce vertical migration patterns. Table 2 shows the definition of formation names and the assigned facies definitions for each formation unit, Table 1 lists the formation names and the assigned rock types (all of them are PetroMod™ defaults).

Note that the facies definitions available in PetroMod™ only describe its petrophysical properties and not its quality as a source rock. The source rock properties are defined via the

TOC and HI values, which are listed here in Table 4. Therefore, the prime source rock of the Vulcan Sub-basin, which is L.Vulcan(sq4a) is defined here as an organic lean and sandy shale, simply because the petrophysical properties of such a facies are closer to the facies defined in the original model (Sandstone 20%, Shale 80%). In a test run, in which pure shale properties were assigned to the Lower Vulcan source rock, only insignificant differences throughout space and time in terms of generated volumes (per Ma) were observed.

Table 1 Formation names and PetroMod™ default lithologies assigned for each formation unit.

Formation Name	Facies Definition
Pliocene	Limestone (shaly)
Miocene	Limestone (shaly)
Eocene	Limestone (shaly)
Paleocene	Limestone (shaly)
U_Cret_(Puffin)	Sandstone (clay rich)
U_Creta_SS75%	Sandstone (clay poor)
U_Creta_SS50%	Sandstone (clay rich)
L_Cretaceous	Shale (organic rich, typical)
L_Creta_SS50%	Sandstone (clay rich)
U_Vulcan(sq-4c)	Shale (organic lean, sandy)
L_Vulcan_U(sq-4b)	Shale (typical)
L._Vulcan_L(sq 4a)_(Montarra)	Shale (organic lean, sandy)
L._Vulcan_L(sq-4a)_SW	Shale (organic lean, sandy)
Plover_Res	Sandstone (typical)
Plover_SR	Shale (organic lean, sandy)
Plover_nil-SR	Sandstone (typical)
M_Jura_and_Triassic	Sand50Shale50

Table 2 Correlation of formation names ands facies definitions.

Period	Formation Name	Deposition [Ma] from	to	Facies 1	Facies 2	Facies 3
NEOGENE	Pliocene	7	0	Pliocene		
	Miocene	34	7	Miocene		
PALAEOGENE	Eocene	56	34	Eocene		
	Palaeocene	65	56	Palaeocene		
CRETACEOUS	U_Cret_Puffin	100	65	U_Cret_(Puffin)	U_Creta_SS75%	U_Creta_SS50%
	L_Cretaceous	136	100	L_Cretaceous	L_Creta_SS50%	
Late - Middle JURASSIC	U_Vulcan(sq 4c)	144	136	U_Vulcan(sq-4c)		
	L_Vulcan_U(sq4b)	150	144	L_Vulcan_U(sq-4b)		
	L._Vulcan_L(sq 4a)_Montarra	163	150	L._Vulcan_L(sq 4a)_(Montarra)	L._Vulcan_L(sq-4a)_SW	
	Plover_Sand1	163.9	163	Plover_Res		
	Plover_SR	164.71	163.9	Plover_SR		
	Plover_Sand2	169.96	164.71	Plover_Res		
	Plover_Shale	171.27	169.96	Plover_nil-SR		
	Plover_Sand3	172	171.27	Plover_Res		
M_Jura and Triassic		250	172	M_Jura_and_Triassic		

Source Rocks

Edwards et al. (2004) investigated the geochemical characteristics of the hydrocarbons from the Vulcan Sub-basin. In summary (Table 3), they recognized two groups (Group A and B) of oils and condensates, and three groups of gases (Groups 1, 2 and 3) from their isotopic profiles. The hydrocarbons are derived from at least two petroleum systems:

- Group A - Lower Vulcan source rock: The Late Jurassic marine Lower Vulcan Formation, the main source for most of the petroleum accumulations in the Vulcan Sub-basin (Edwards et al., 2004; Kennard et al., 1999)

- Group B - Plover source rock: The coal-rich Early to Middle Jurassic Plover Formation, which is thought to be the secondary source rock in the Vulcan Sub-basin. At the flanks of the Cartier Trough the formation contains organic-rich mudstones with fair to very good source properties (Edwards et al., 2004).

Well data from Leewin, Tenacious, Audacious, Padthaway, Crux and Bilyara were not supplied by GA for the numerical model; their locations are shown in Figure 3. Note that the other figures do not show those locations, as the data for those wells was added upon request by GA after modelling.

Table 3 Vulcan Sub-basin source-related petroleum groups (Edwards et al., 2004). More wells which are not listed here have hydrocarbon shows. g/c: gas & condensate; g/o: gas & oil.

Well/Field	HC	Gas Group	Oil Group	°API	GOR (scf/stb)	Inferred source rock
Leeuwin-1	gas	1	?	?	?	unknown
Swan-1,3	gas	1	A+?	40-55	?	Lower+Upper Vulcan?
Tahbilk-1(2,690.2m)	g/c	1	A	?	?	Lower Vulcan+Plover?
Cassini-1	g/o	2	A	40	250	Lower Vulcan
Tahbilk-1(2,305m)	g/c	2	A	?	?	Lower Vulcan
Skua-2,3,4,5,8,9	g/o	2	A	?	700-2000	Lower Vulcan
Birch-1ST1	oil	?	A	43	222	Lower Vulcan
Challis-1,3,7,8	oil	?	A	40	326	Lower Vulcan
Eclipse-2	g/o	?	A	30-49	?	Lower Vulcan
Jabiru-1A,8A,11	oil	?	A	42.5	260-350	Lower Vulcan
Octavius-1	oil	?	A	37.5		Lower Vulcan
Talbot-1,2	oil	?	A	50		Lower Vulcan
Tenacious-1	oil	?	A	49	520	Lower Vulcan
Audacious-1	oil	?	A+?	55	264	Lower Vulcan
Puffin-1,2,3,5	oil	?	A+?	45	105-197	Lower Vulcan +?
Pengana-1	g/c	3	A+?	45	?	Lower Vulcan +?
Oliver-1	g/o	3	A+B	31.8	628	Lower Vulcan + Plover?
Montara-1, 2	g/o	2	B	34.6	324	Plover?
Padthaway-1	g/c	2	B	34.6	3613	Plover?
Crux-1	g/c	3	B	53.7	?	Plover?
Maple-1	g/o	3	?	?	?	Plover?
Bilyara-1 ST1	oil	?	B	37	976	Plover?
Maret-1	condensate	?	B	39.7	?	Plover coal

Differences in timing of generation from the individual source rocks and in migration patterns result in the mixed hydrocarbon accumulations seen at several locations throughout the Vulcan Sub-basin. The regional distribution of the groups is shown in Figure 2.

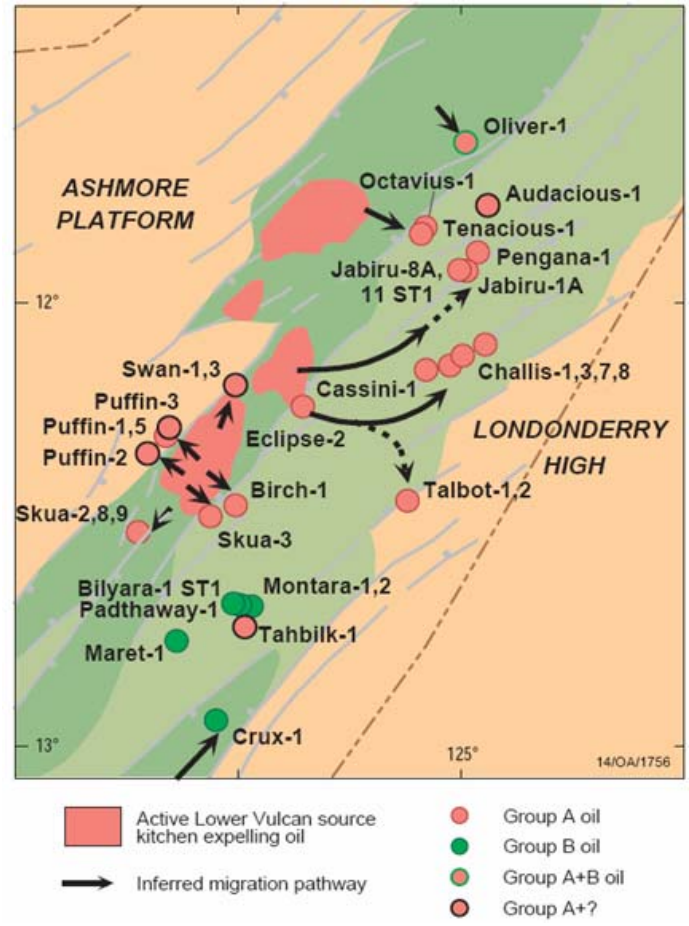

Figure 2 Inferred migration pathways of the Vulcan Sub-basin Group A and B oils and condensates (from Edwards et al (2004), modified after Chen et al., 2002).

The majority of oils and condensates from the Vulcan Sub-basin have a mixed marine and terrestrial geochemical signature (Edwards et al., 2004). In order to reproduce this pattern both source rocks were taken into account, where for each source rock interval, HI and TOC values were assigned to the numerical models as discussed with GA and listed in Table 4.

The main problem with the determination of phase predictive compositional kinetic schemes using conventional pyrolysis methods lies in the determination of gas compositions. While pyrolysis methods accurately reconstruct hydrocarbon GORs they are incapable of correctly reproducing the gas composition of natural fluids. As the gas composition dominantly controls the phase behaviour of petroleum multi-compound compositional kinetic predictions based on pyrolysis results alone are inappropriate for the prediction of phase behaviour. A method developed by di Primio and Horsfield (2004) uses a combination of open and closed system pyrolysis techniques to characterize the compositional evolution of the fluids generated as a function of increasing thermal stress. Gas compositions determined analytically are iteratively tuned to natural fluid phase behaviour and the ensuing “corrected” gas compositions used for the definition of multi-compound kinetic models.

Following this approach compositional kinetic models for the Lower Vulcan and the Plover formations were developed. The properties of the compositional kinetics of the Lower Vulcan and the Plover formations (Table 4) are described in detail in the report previously prepared by GeoS4 GmbH for Geoscience Australia on selected samples from the Vulcan Sub-basin.

Table 4 Source rock properties assigned in the digital models.

Source Interval	TOC	HI	Assigned Kinetics
L._Vulcan_L(sq 4a)_(Montarra)	1.6	200	G005732 4-Comp_Crack
L._Vulcan_L(sq-4a)_SW	0.7	150	G005732 4-Comp_Crack
Plover_SR	3	215	G005733 4-Comp_Crack_Plover

In the present study the 4-compound kinetic models were used, which accurately reproduce petroleum GOR evolution as well as the physical properties of the fluids at lower computational cost than if the PhaseKinetic models were used, which contain 14 compounds. For detailed phase behaviour calculations as well as for the simulation of petroleum alteration it is, however, recommended to use the full PhaseKinetic definitions. Details on the comparability of 4- and 14-compound model predictions are listed in Appendix 2. There also the cracking models implemented are discussed.

In addition to the characterization of primary cracking products described by the compositional kinetic models, secondary cracking of the primary generated compounds was also defined. The secondary cracking of hydrocarbons has been investigated experimentally in detail (Dieckmann et al., 1998; Horsfield et al., 1992; Schenk et al., 1997). While the stability of hydrocarbons in reservoirs is relatively high, onset of in-reservoir cracking starts at reservoir temperatures of 180-200°C at geologic heating rates (Dieckmann et al., 1998; Horsfield et al., 1992), the cracking of residual hydrocarbons in the source rock environment occurs at significantly lower geologic temperatures, i.e. starting already at roughly 150°C (Dieckmann et al., 1998). In the experimental studies listed oil cracking was described by the formation of gas (C1-5) due to the cracking of the C6+ petroleum fraction. For the compositional kinetic models applied here the use of two compounds describing the liquid composition precluded the definition of oil cracking using a single bulk reaction characterization. The definition of secondary cracking used is described in the PhaseKinetics report 20080818 from GeoS4 and in Appendix 2. The kinetic models of primary cracking applied are shown in *Table 14*. Methane was defined as the single compound being produced from oil cracking.

The expulsion model standardly implemented in PetroMod is based on a saturation threshold. This is a petrophysical parameter and therefore set for each lithology separately. The default setting is 1% for oil and 0% for gas. In the implemented 4-compound kinetic models including secondary cracking, however, an adsorption based model is used to calculated expulsion. In this case the dead carbon proportion of the source rock adsorbs generated hydrocarbons. Only when the sorptive capacity is exceed is expulsion possible. This approach follows the Pepper and Corvi (1995) model. The only variation is that a whole-phase adsorption model is used as compared to a two-phase adsorption model in Pepper and Corvi (1995). Based on the source rock properties listed in Table 4 dead carbon contents of the Vulcan and Plover source rocks are high, reaching values of 76 to 82% of the total organic carbon (see source rock kinetics in PetroMod format of GeoS4 report 20080818). Accordingly, a relatively large retention capacity of these source rocks has to be assumed. The application of this expulsion model based on the adsorptive capacity of the kerogen results in

relatively high degrees of kerogen conversion being required before expulsion occurs. Application of the standard PetroMod saturation-based expulsion model would have resulted in significantly earlier expulsion times. However, the PhaseKinetic modelling approach applied here is only applicable using the modified adsorption based expulsion model of Pepper and Corvi (1995) when secondary cracking is to be taken into account. As stated by IES Germany (Hantschel pers. com.) PetroMod expulsion times are not very reliable, since they depend on a variety of variables the contributions of which are difficult to assess individually and are averaged over an area. Accordingly a relatively large error margin of this output information should be taken into account in the discussion of expulsion times.

In the present study the individual components of the two source rock kinetic models used were tagged in order to be able to identify relative contributions to any given accumulation. Hydrocarbons generated by the Vulcan Formation are named according to the usual 4-compound definition, i.e. Methane, C2-C5, PK_C6-C14 and PK_C15+. The Plover Formation products are characterized by the suffix Pl_, i.e. Pl_Methane, Pl_C2-C5, etc.

The geographic distribution of the known source rock intervals shown in Figure 3 were proposed by GA and assigned to the numerical models. In the south-western area of the Vulcan source rock facies map (Figure 3) a facies was assigned with the same rock properties but distinctively lower TOC and HI values as compared to the facies assigned to the rest of the area. This facies occurs in the structural saddle between the Swan Graben to the north and the Browse Basin to the south, and was necessary in order to reduce the volume of generated petroleum in that area. The assigned compositional kinetic models are identical for both.

The reserves of the Vulcan-Sub-basin are estimated to be 357 MMbbls oil, 31 MMbbls condensates and 1.3 Tcf gas or 58/5/36% oil/condensate/gas volume split respectively by boe (Longley et al., 2002).

A full assessment of the masses generated, expelled, cracked and accumulated could not be made for the present study due to incorrect data extraction routines in PetroMods PetroReport program which was identified during this study and is described in detail in the Summary and Conclusions.

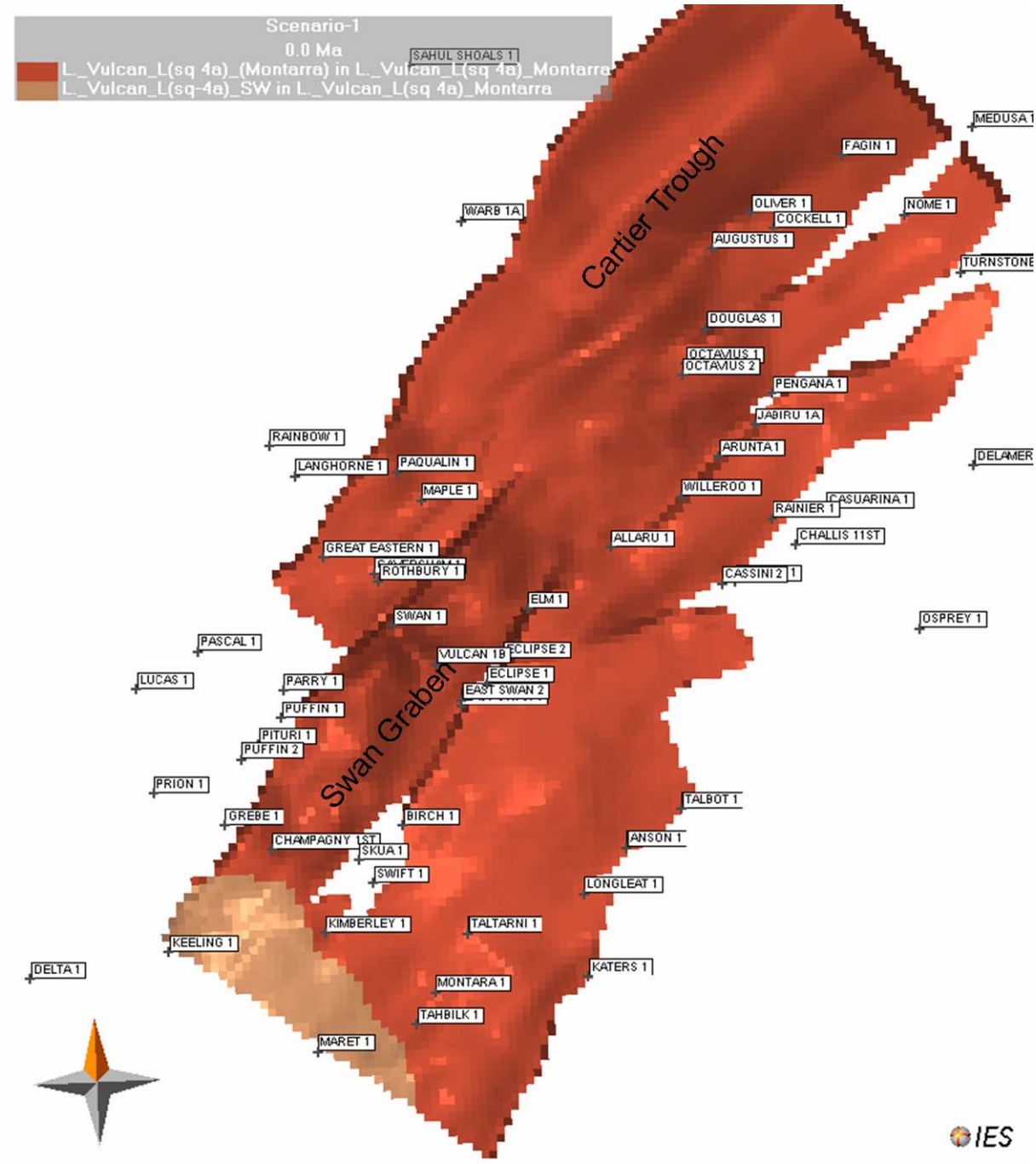

Figure 3 Distribution of the Lower Vulcan source rock facies.

Seal Properties

Jurassic intra-formational shale and claystone seals are described by Bradshaw and co-workers (1994). Local and regional seal rocks are lower to upper Cretaceous (Valaginian-Cenomanian) claystones. Kivior et al. (2002) studied the seal potential in Cretaceous and Late Jurassic rocks of the Vulcan Sub-basin.

To simulate a rather leaky sealing formation, the seal properties of the Upper Vulcan (seq-4c) and the L_Cretaceous formations were adjusted in the Lithology Editor. Capillary entry pressures for the upper Vulcan seal were reduced in order to remove accumulations at the graben margin (*Figure 4*). The leaky lithology was assigned to the facies in scenario 4.

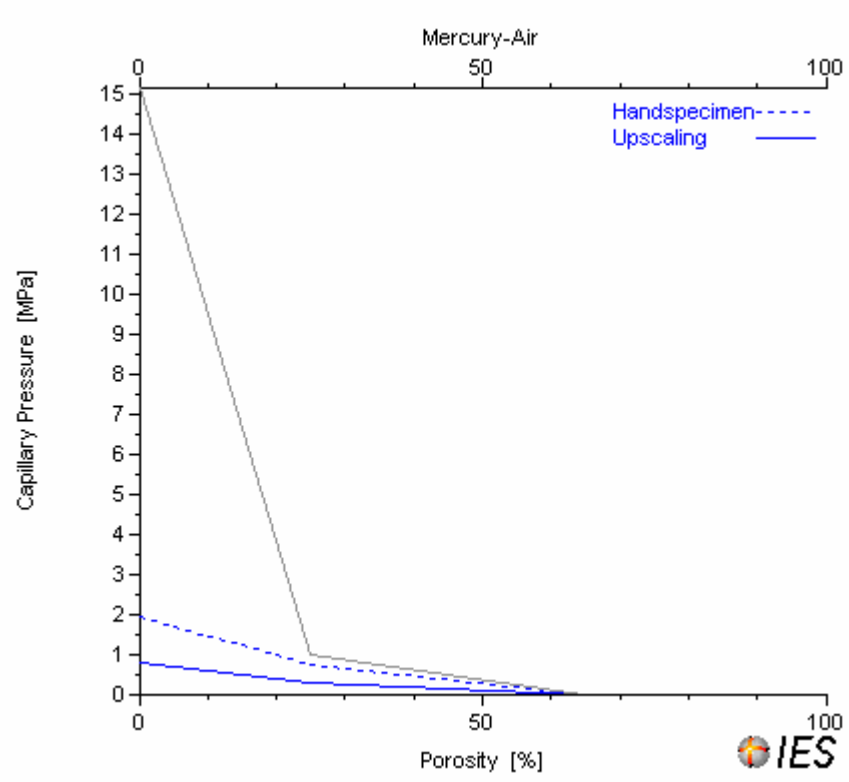

Figure 4 Seal properties used for the sealing lithologies in some of the modelled scenarios. The blue graphs show the definitions used for the leaky seal scenarios.

Description of Modelling Scenarios

GA required a set of scenarios to be modelled. The variations of the numerical set-ups are listed below in Table 6. The modelled scenarios differ in the assignment of the source rock properties and compositional kinetics. In two scenarios no source rock properties and no compositional kinetic model were assigned to the Plover Formation (scenario 1 and 2). This scenario was included in order to better constrain the contribution of petroleum generated by the Lower Vulcan source rock interval. Scenarios 3 and 4 take the Plover Formation as a contributing source rock interval into account. Three of the modelled scenarios include a variation in TOC and HI for the most south-western area of the Lower Vulcan Formation (scenarios 2, 3 and 4). Kivior et al. (2002) studied the seal potential in Cretaceous and Late Jurassic rocks of the Vulcan Sub-basin. They concluded that top seal capillary failure is rather unlikely to be mechanism for hydrocarbon leakage. However, in order to handle the leakage numerically, variations of the sealing capacity of the upper Vulcan seal were modelled in order to remove accumulations at the graben margin (scenario 4).

In Scenario 5 (copy of Scenario_3), faults which were part of the original model, were assigned to the formations between the M_Jura and Triassic up to the U_Vulcan (seq4c). Three main faults (SwanGNW, SGSE and CTNW0) were extended up into the U_Cret_Puffin horizon. The fault model available in PetroMod™ allows changes over time in the faults transmissibility. Migration was allowed along the faults during rifting periods (163-136 Ma; Miocene reactivation of three selected main faults between 6 to 0 Ma). The fault assignment is shown in Table 5. The definitions of the different fault properties of PetroMod™ are in summary: The fault capillary pressure describes the resistance of the fault for fluid flow, the higher the value, the less permeable is the fault (100 MPa makes the fault impermeable). The “closed” fault type closes the fault with respect to fluid flow (sealing fault); the “open” fault type opens the fault with respect to fluid flow (leaking fault), “none” types are ignored during the specific time interval of the simulation. A more detailed description about fault properties is given in Yielding et al., (1997).

Table 5 Fault properties

Fault Name	Fault Type	Fault Capillary Pressure (Mpa)	From (Ma)	To (Ma)	Fault Type	Fault Capillary Pressure (Mpa)	From (Ma)	To (Ma)	Fault Type	Fault Capillary Pressure (Mpa)	From (Ma)	To (Ma)
CTNW	open	10	163	136	closed	100	136	0	none	0	0	0
SwanGNW	open	10	163	136	closed	100	136	6	open	10	6	0
CTSE	open	10	163	136	closed	100	136	0	none	0	0	0
CTSE2	open	10	163	136	closed	100	136	0	none	0	0	0
JHNW	open	10	163	136	closed	100	136	0	none	0	0	0
JHSE	open	10	163	136	closed	100	136	0	none	0	0	0
JTSE	open	10	163	136	closed	100	136	0	none	0	0	0
CTNW0	open	10	163	136	closed	100	136	6	open	10	6	0
SwanGNW2	open	10	163	136	closed	100	136	0	none	0	0	0
CTS	open	10	163	136	closed	100	136	0	none	0	0	0
SGSE	open	10	163	136	closed	100	136	6	open	10	6	0
PGS	open	10	163	136	closed	100	136	0	none	0	0	0
PGSS	open	10	163	136	closed	100	136	0	none	0	0	0
PHNW	open	10	163	136	closed	100	136	0	none	0	0	0
CTSS	open	10	163	136	closed	100	136	0	none	0	0	0

Table 6 Set-up of the numerical models.

Model	Settings
Scenario 1	• Lower Vulcan
Scenario_2	• Lower Vulcan • Lower Vulcan_SW • Reduced capillary entry pressure for upper Vulcan
Scenario_3	• Lower Vulcan • Lower Vulcan_SW • Plover
Scenario_4	• Lower Vulcan • Lower Vulcan_SW • Plover • Reduced capillary entry pressure for upper Vulcan
Scenario_5	• Lower Vulcan • Lower Vulcan_SW • Plover • Faults assigned

Simulation

Once the numerical model includes the required set of input data, the simulation starts. To reduce processing time an eight node (8 GB RAM per node) Linux based PC cluster for parallel processing was used. During the simulation, the geological evolution of the basin through time, including its thermal and pressure history, is reconstructed. Simulation is an iterative process, which means that it will be repeated until a satisfying result is achieved, using the results of the previous runs as first approximations.

In order to assess the migration histories of both areas, first the drainage areas and subsequently the migration paths of the generated hydrocarbons were modelled.

The carrier maps were divided into drainage areas by the PetroMod's PetroCharge tool, which models migration as flow within a defined carrier. The calculated drainage area borders, the closures, showing areas of possible hydrocarbon accumulations and the calculated spill paths, are based on the layers topography. Migration is assumed to occur instantaneously. Such flowpath models are based on the assumption, that

- petroleum flows against a defined surface (e.g. a regional seal),
- migration is only buoyancy driven (IES, 2002).

The following options were chosen within the Simulator module of PetroMod™:

- The chosen petroleum migration method for the simulation is the Hybrid Model, which combines both Darcy flow and Flowpath.
- The reservoir definition has a threshold value of 10^{-2} mD permeability at 30% porosity (sedimentary units with values equal to or higher than this permeability at 30% porosity are assumed to be carriers).
- Migration within units which did not match the criteria for carriers was modelled assuming Darcy flow.
- The chosen adsorption model is the "expelled composition" model. For details on the cracking model applied see Appendix 2.
- Equation of State: Peng Robinson.

- The model's basin sides were left open in all simulation runs, generated petroleum migrating to the model's margins could therefore leave the basin through the open sides, thereby preventing artificially trapped accumulations in the model boundaries.

As the input data set contained undefined values (99999) at several locations within the numerical model (which resulted in holes (no data) in the output results throughout all layers of the entire model at that location), those values were removed by setting them to 0, thereby defining a zero thickness which closed the data gaps throughout the model.

Results

Initial thermal modelling of the study area indicated that no differences regarding calibration were obvious between the V.9 and V. 10 models. Accordingly the thermal history definition as described by Fujii et al. (2004) applies also to the models presented here. The following section describes the results of the different source rock scenarios under the assumption that the geographic distribution of the different source rock facies and the assigned properties as determined by GA are correct.

All modelled scenarios predict hydrocarbon accumulations or traces to be present in the following formations:

- U_Cret_Puffin (traces/ small accumulations, e.g. at Langhorne 1)
- L_Cretaceous (traces)
- Plover_Sand1 (main reservoir unit)
- Plover_Sand2 (traces/ small accumulations, e.g. at Jaribu 1A)
- Plover_Shale (traces)
- Plover_Sand3 (traces)

However, it is only the Plover_Sand1 which contains economically interesting volumes of hydrocarbons.

Scenario 1

This scenario considers only the source rock potential of the Lower Vulcan Formation with no potential in its south-western area. The regional distribution of the presently transformed organic matter is shown in *Figure 5*. *Table 7* compares the fluid properties of the modelled hydrocarbon accumulations to the ones reported in Edwards et al. (2004).

Table 7 Field data (Edwards et al., 2004) and the modelled results.

	Edwards et al. (2004)			Scenario_1		
Well/Field	**°API**	**GOR (stb/scf)**	**HC Type**	**°API**	**GOR (stb/scf)**	**HC Type**
Leeuwin-1	?	?	gas	-	-	No accum.
Swan-1,3	40-55	?	gas	54	110000	g/c
Tahbilk-1	?	?	g/c	23	612	g/c
Cassini-1	40	250	g/o	56	1200	oil
Skua-2,3,4,5,8,9	?	700-2000	g/o	32	1540	g/o
Birch-1ST1	43	222	oil	34	12500	g/o
Challis-1,3,7,8	40	326	oil	57	1650	traces
Eclipse-2	30-49	?	g/o	55 (32)	22000 (234)	g (o)
Jabiru-1A,8A,11	42.5	260-350	oil	27	860	g/o
Octavius-1	37.5		oil	-	-	-
Talbot-1,2	50		oil	23	611	oil
Tenacious-1	49	520	oil	-	-	No accum.
Audacious-1	55	264	oil	28	892	oil
Puffin-1,2,3,5	45	105-197	oil	27	1050	g/o
Pengana-1	45	?	g/c	27	860	oil
Oliver-1	31.8	628	g/o	-	-	-
Montara-1, 2	34.6	324	g/o	-	-	-
Padthaway-1	34.6	3613	g/c	23	606	oil
Crux-1	53.7	?	g/c	-	-	-
Maple-1	?	?	g/o	29	966	g/o
Bilyara-1 ST1	37	976	oil	-	-	-
Maret-1	39.7	?	condensate	-	-	-

The compositional kinetic models predict petroleum accumulation for a variety of formations, with the Plover Formation being the main reservoir unit and the Puffin Formation being the secondary. The predicted petroleum accumulations in the Plover Sand 1 west of Montara 1 at Padthaway 1 (~10 MMbbls) and Tahbilk (~45 MMbbls) wells are rather small (*Figure 6*). The migration paths which are visible in *Figure 6* in the south-western non-source area originate from the active kitchen outside the non-source area (transparent overlay in the south-west of *Figure 6*). The predicted oil accumulation at the Swift/Skua location is also small (~12 MMbbls). The migration pathways east of Douglas point towards the Audacious well, which is located approximately 20 km east of Douglas, and confirm known accumulations at that structure. Oil was modelled to be present within the Jaribu structure.

According to GA, the Plover sand is absent in the Maple and the Cassini structures, but provides the carrier to the structures, where the model predicts accumulations to be present.

Within the Lower Cretaceous Puffin Formation, the assigned compositional model for the Vulcan Formation predicts oil accumulations for the Puffin structure (*Figure 7*).

Figure 8 shows the predicted transformation ratio evolution through time for the Lower Vulcan source rock unit. The assigned compositional kinetic models predict the onset of petroleum generation for the deepest location of the formation (the Swan Graben) at the end of the Late Jurassic at 145 Ma. Transformation is not completed yet.

As stated in earlier, is the application of this expulsion model based on the adsorptive capacity of the kerogen results in relatively high degrees of kerogen conversion being required before expulsion occurs. This is obvious in Figures 8 and 9 where transformation ratios of over 40-60% are required (depending on the source rock characteristics) before expulsion (as expressed by the line “Expulsion time”) occurs. More specifically, the expulsion of petroleum occurred at approximately 100 Ma at the Swan Graben location shown in *Figure 5*.

Based on the applied PhaseKinetic models of hydrocarbon generation, expulsion and cracking organic matter within the Cartier Trough in the North of the basin has reached up to 80% conversion (*Figure 9*). The onset of petroleum generation here occurred in the Early Cretaceous, at 140 Ma. Subsequent generation occurred during the Oligocene, followed by a sharp drop and an increase during the last 8 Ma. Expulsion time was at 7 Ma.

Results in terms of cumulative hydrocarbon volumes as reported for the petroleum systems are shown in the Appendix. The data is available in digital format in the PetroReport module of this scenario. *Figure 10* summarizes the total cumulative volumes of hydrocarbons which were generated, expelled and accumulated. Here it should be taken into account that unexpelled petroleum as well as residual petroleum saturations are included in the “accumulated” volumes. Additionally, due to an error in the PetroReport extraction routine “expelled volumes” are incorrect. This data could, however, not be removed from the graphics as a user-defined output graphic is not available for this option in PetroMod.

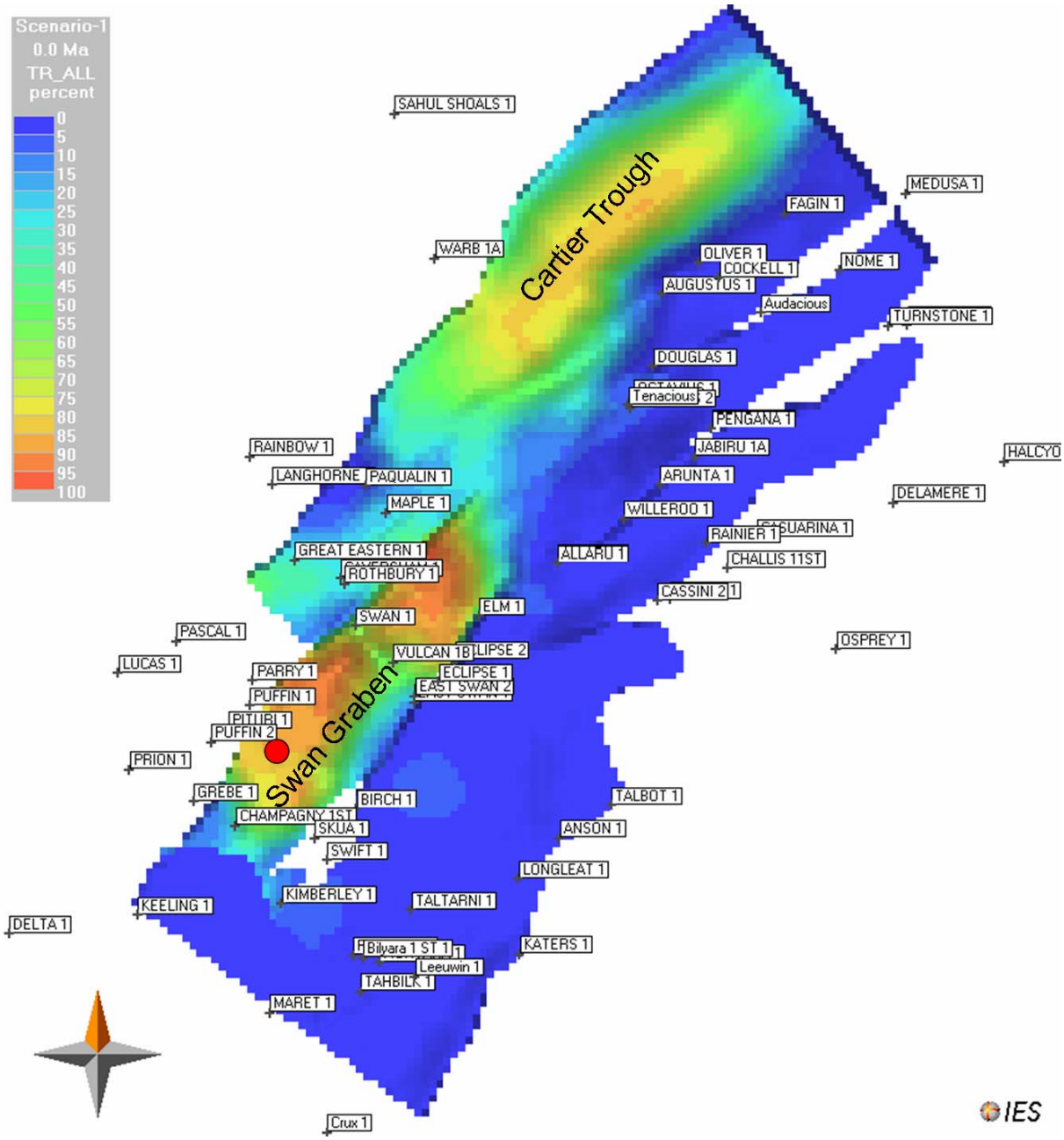

Figure 5 Present day Lower Vulcan source rock. Overlay is transformation ratio; oil and gas flow vectors (green/red) are included, the red dots show the locations for the 1D time shots (Figure 8 and Figure 9).

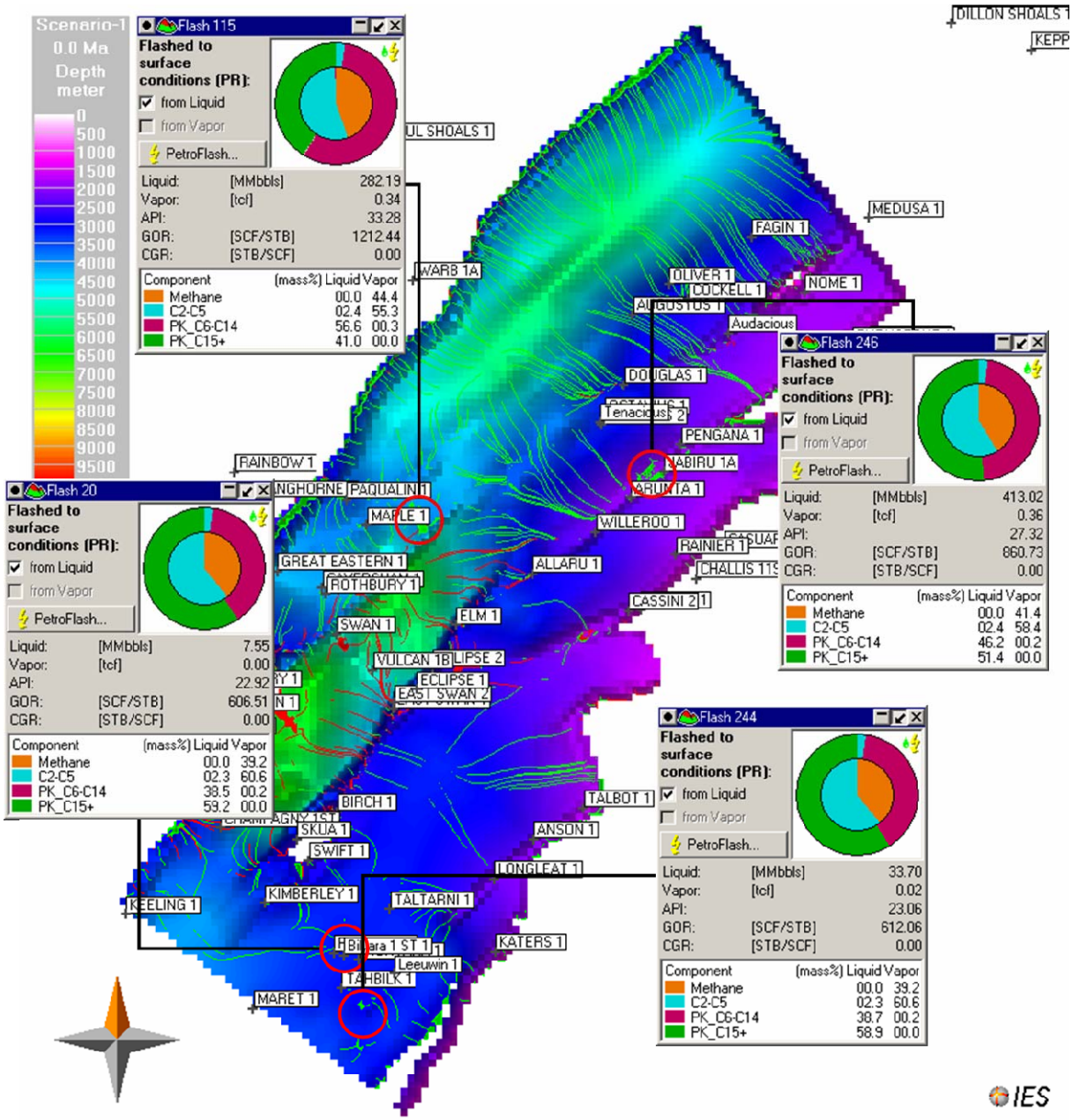

Figure 6 Oil and gas accumulations and flow paths (green/red) in the uppermost Plover Sand_1 (present day, colour overlay is depth). Green and red circles show successfully reproduced oil and gas accumulations. The pie diagram shows the compositions of the fluid encountered east of Maple, west of Montara (Padthaway-1), at Jabiru 1a and south of Tahbilk.

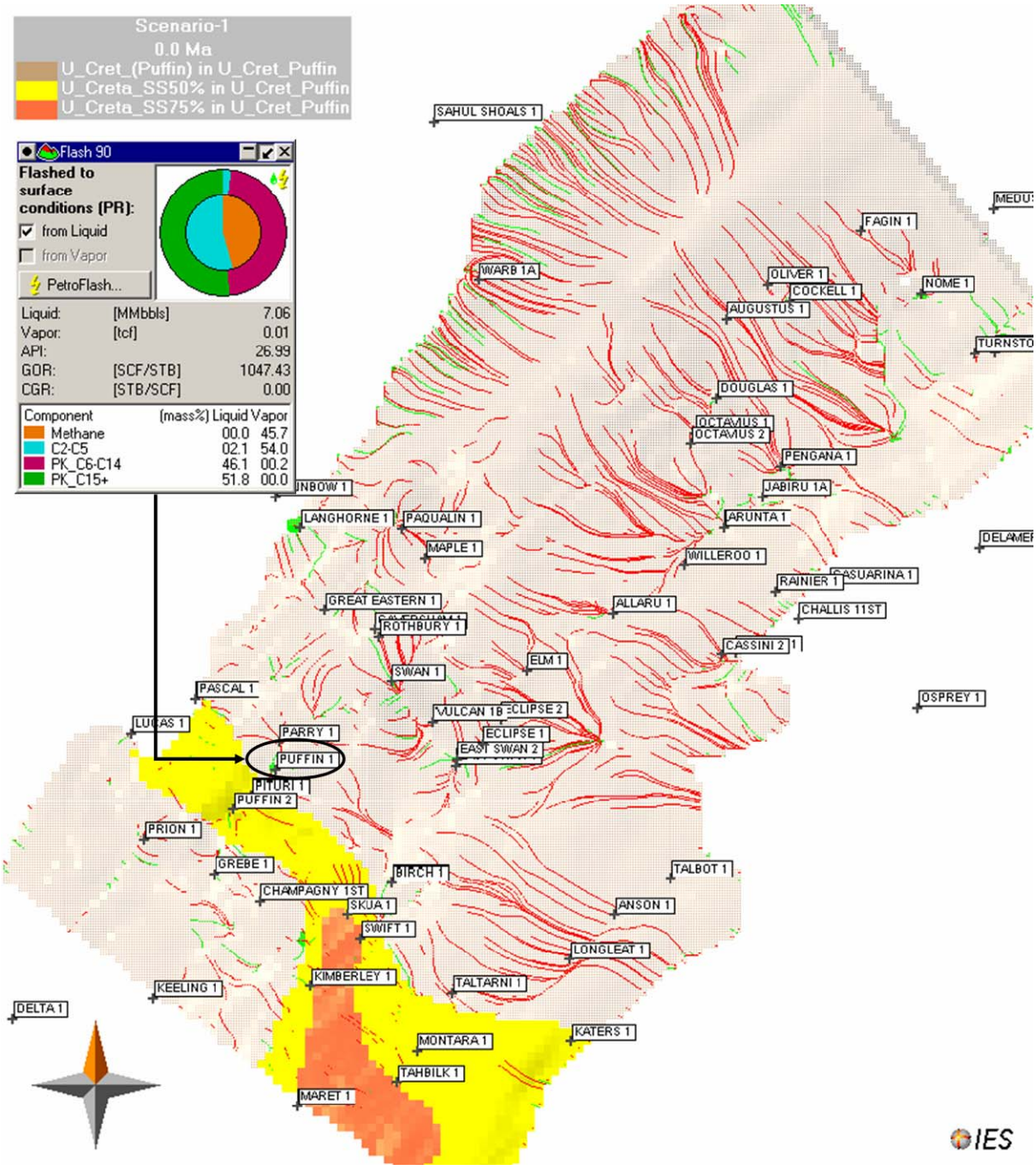

Figure 7 U_Cret. Puffin Formation, present day: Oil (green) and gas (red) accumulations and flow. The pie diagram shows the composition of the fluid predicted at the Puffin well.

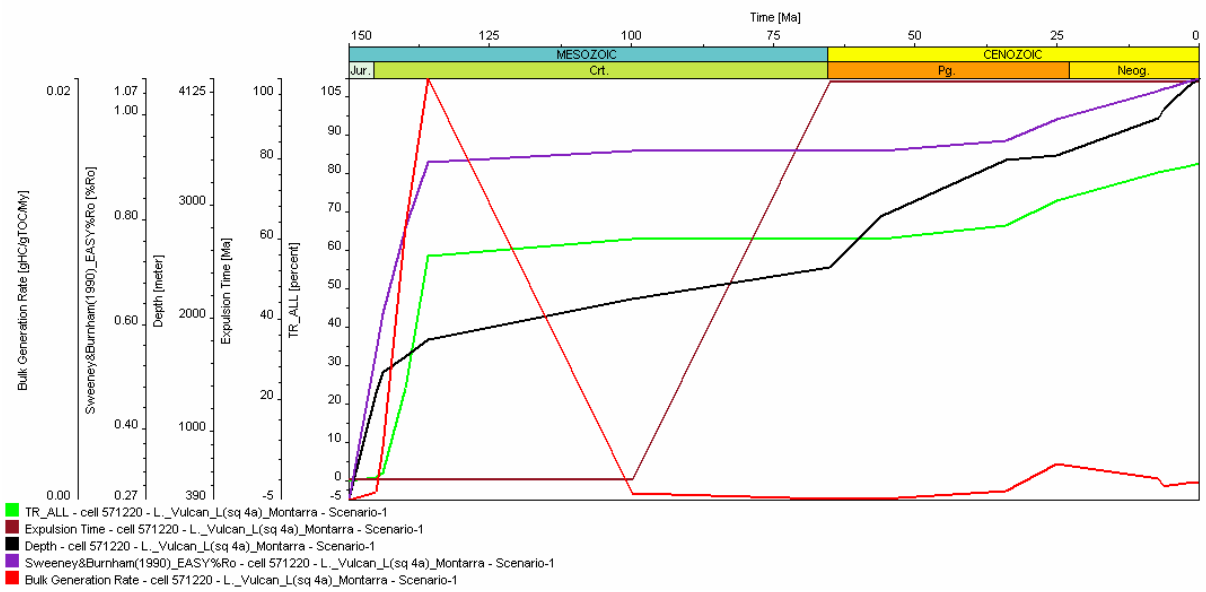

Figure 8 Central Swan Graben, Lower Vulcan Formation: Timing of petroleum generation and expulsion.

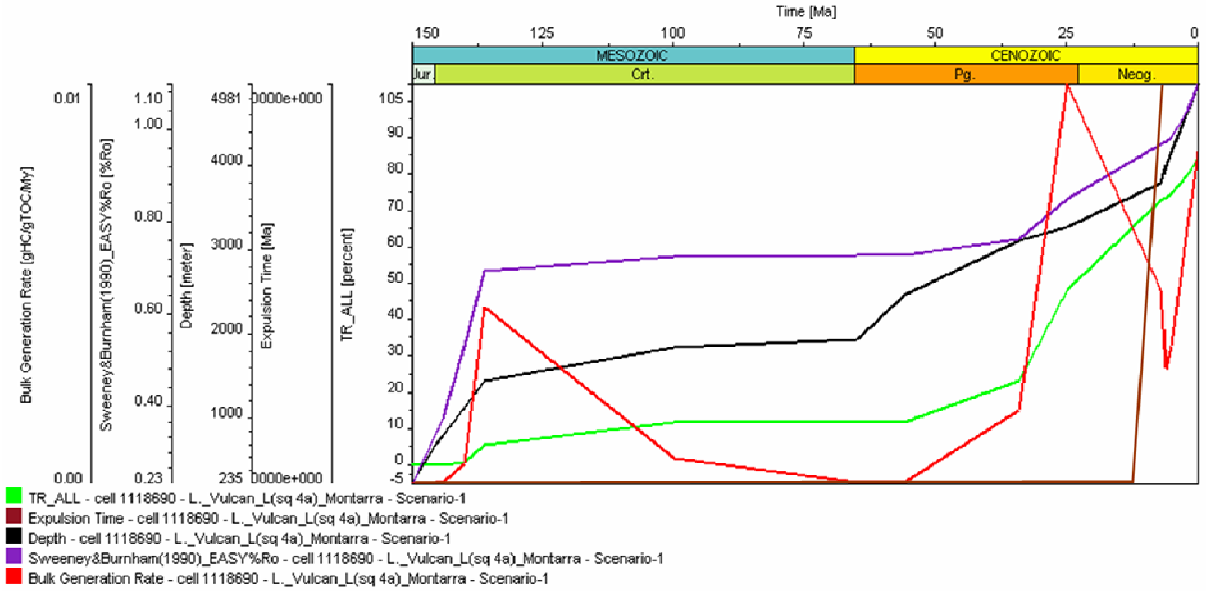

Figure 9 Cartier Trough, Lower Vulcan Formation: Timing of petroleum generation and expulsion.

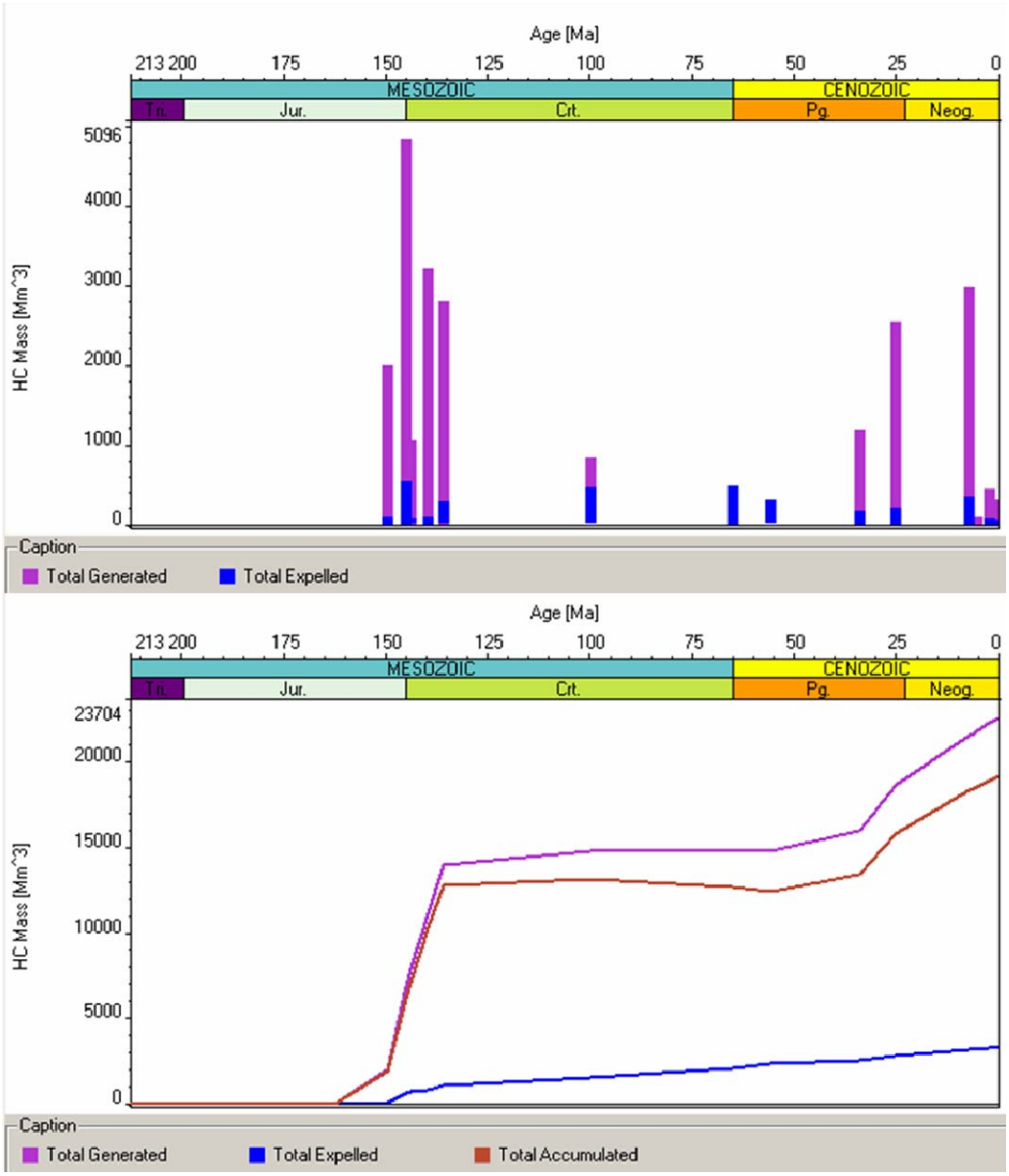

Figure 10 Overview of timing and total volumes of the generated, expelled and accumulated hydrocarbons over time for the entire digital model. Please note that only the generated volumes described here are reliable as discussed in the summary and conclusions.

Scenario 2

This scenario considers the source rock potential of the Lower Vulcan Formation, including its south-western area, although the source rock properties in terms of TOC and HI are here reduced as compared to the rest of this formation.

The additional input of the tested south-western Lower Vulcan source rock potential is evident in the volumetric increase of the accumulations at Padthaway/west of Montara (Scenario 1: ~7 MMbbls, Scenari_2: ~10 MMbbls) and south of Tahbilk (Scenario_1: ~32 MMbbls; Scenario_2: ~56 MMbbls) in the Plover Sand 1 (*Figure 12*). The predicted accumulations in the Lower Cretaceous Puffin Formation (*Figure 13*) are identical to the ones shown in Scenario 1 (Figure 7). API, GOR and fluid type data are ± identical to the results of Scenario_1.

Figure 14 shows the predicted transformation ratio evolution through time for the Lower Vulcan source rock unit at the location shown in *Figure 11*. The assigned compositional kinetic models predict the onset of petroleum generation for the location at 35 Ma. Transformation has not been completed. Presently the transformation of organic matter within the south-western area has reached about 30% with no, or only minimal, expulsion of petroleum, which is basically due to the low TOC and HI values assigned here as well as the high inert carbon content of the kerogen. This observation may seem strange in view of the observed higher volumes of fluids encountered in the Padthaway/ west of Montara and Tahbilk fields in this simulation, is however, easily explained by the fact that the time shot shown in Figure 14 is valid only for the surface of the source rock at the location where the 1D time shot was taken. The base of the source rock in the same location has reached a distinctly higher degree of transformation (70%) and has accordingly also expelled hydrocarbons.

Results in terms of cumulative hydrocarbon volumes as reported for the Petroleum Systems are shown in the Appendix. The data is available in digital format in the PetroReport module of this scenario. *Figure 15* summarizes the total cumulative volumes of hydrocarbons which were generated, expelled and accumulated. Here it should be taken into account that unexpelled petroleum as well as residual petroleum saturations are included in the “accumulated” volumes. Additionally, due to an error in the PetroReport extraction routine “expelled volumes” are incorrect. This data could, however, not be removed from the graphics as a user-defined output graphic is not available for this option in PetroMod.

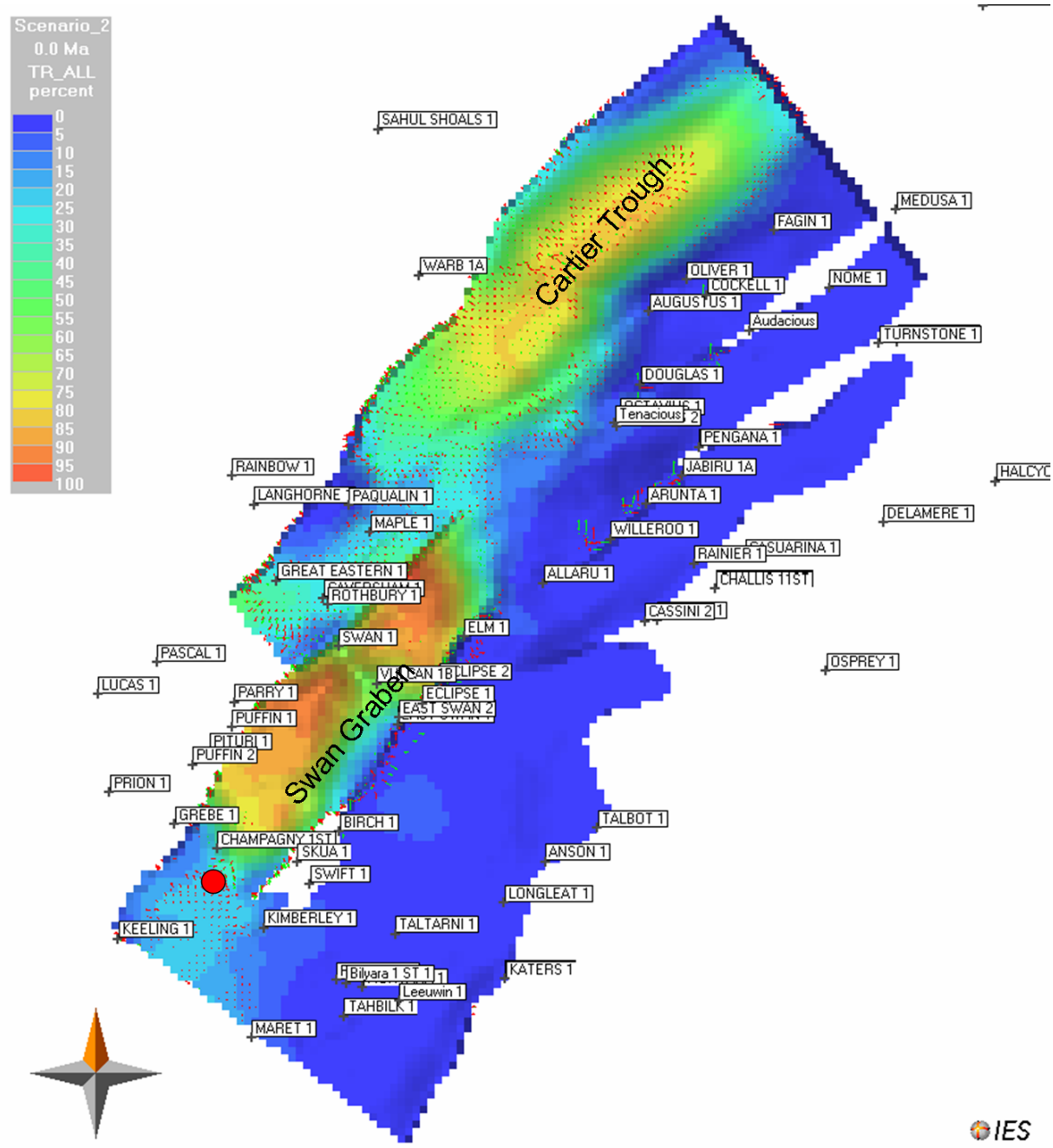

Figure 11 Present day Lower Vulcan source rock. Overlay is transformation ratio; oil and gas flow vectors (green/red) are included, the red dot shows the location for the 1D time shot (Figure 14).

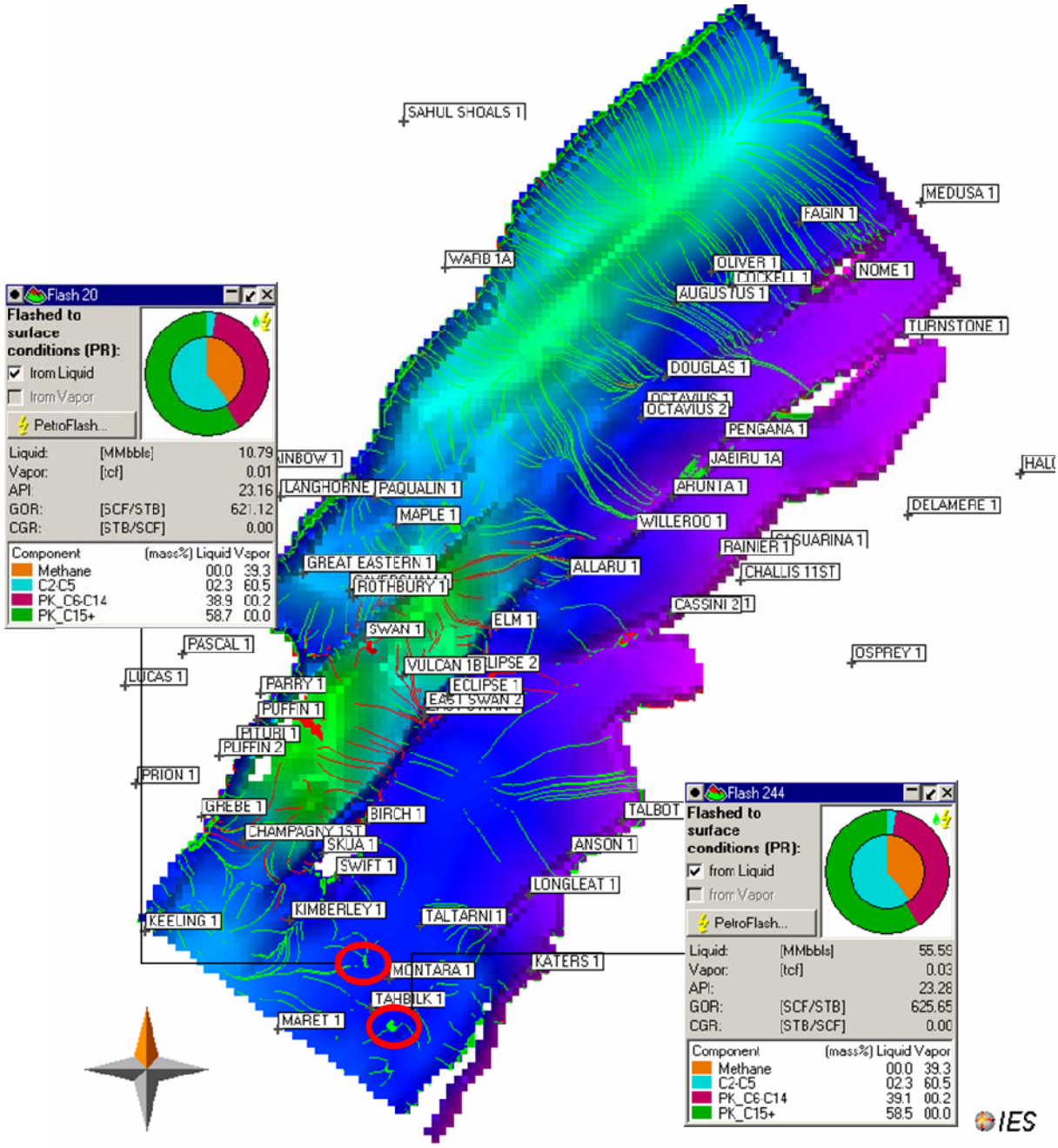

Figure 12 Oil and gas accumulations and flow paths (green/red) in the uppermost Plover Sand_1 (present day, colour overlay is depth). The pie diagram shows the composition of the gas predicted for the Tahbilk and for the Montara structures.

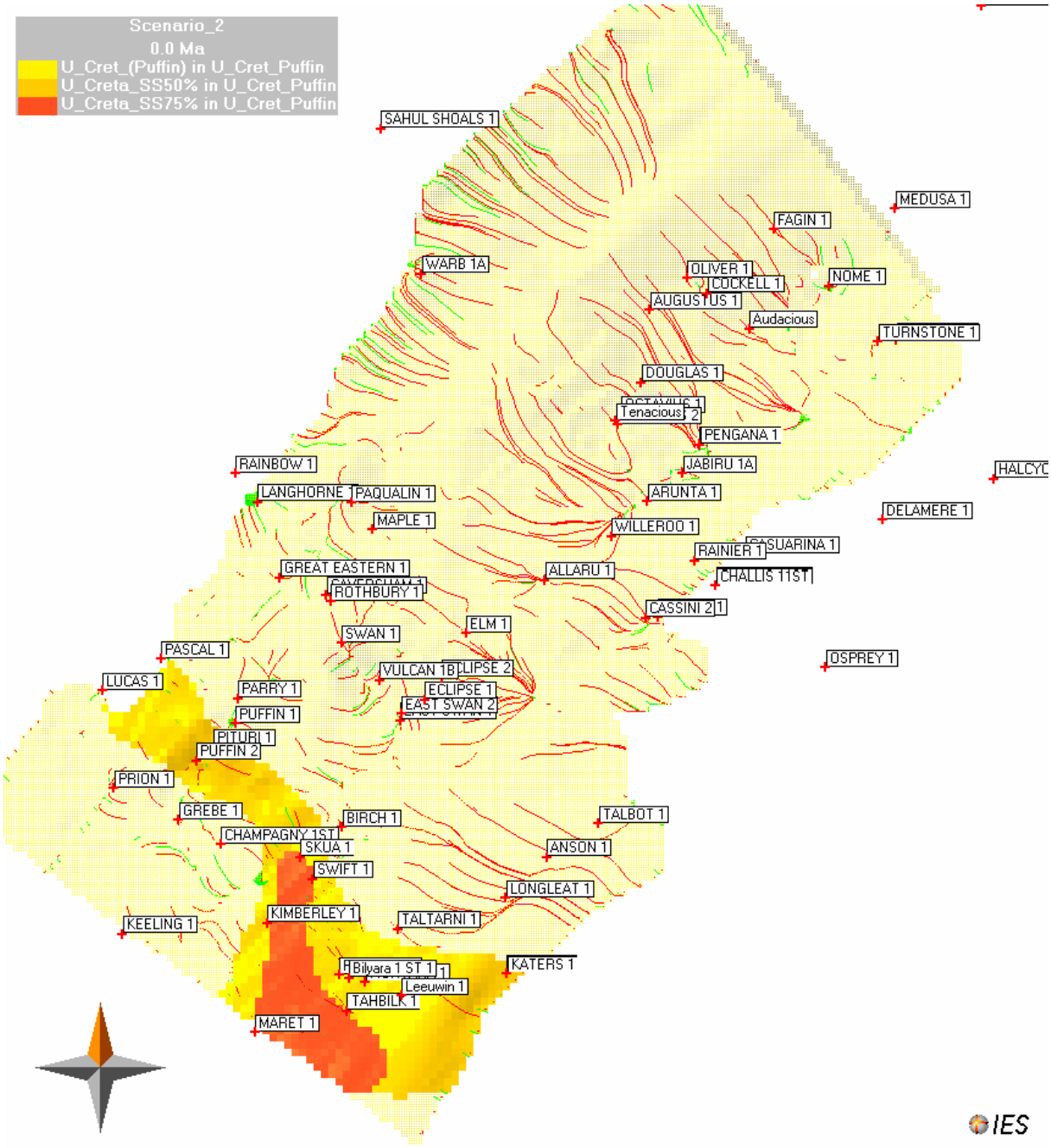

Figure 13 U_Cret. Puffin Formation, present day: Oil (green) and gas (red) accumulations and flow.

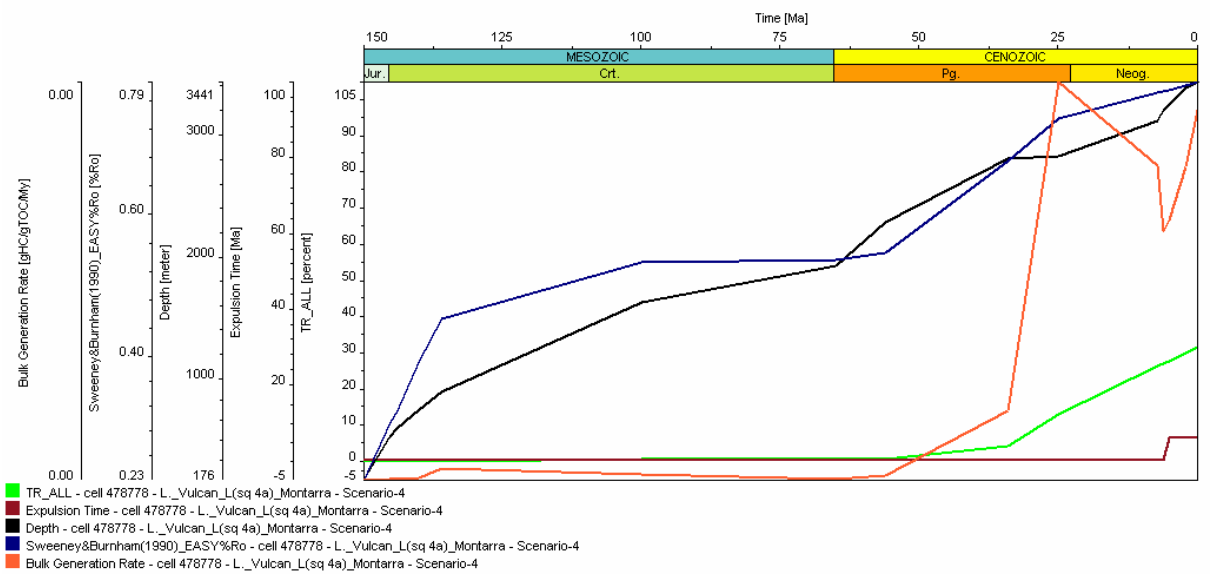

Figure 14 Lower Vulcan Formation, south-western area: Timing of petroleum generation and expulsion.

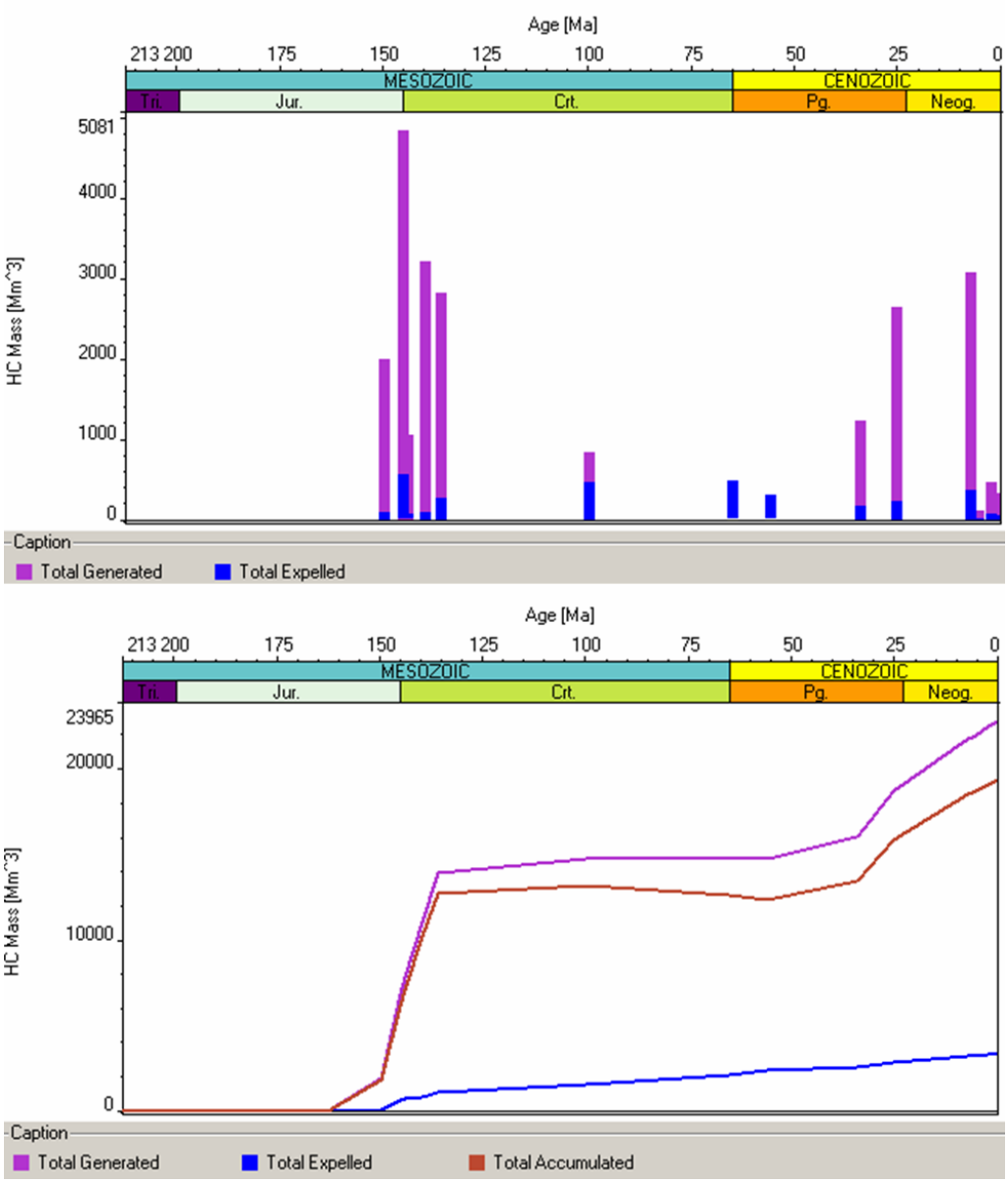

Figure 15 Overview of timing and total volumes of the generated, expelled and accumulated hydrocarbons over time for the entire digital model. Please note that only the generated volumes described here are reliable as discussed in the summary and conclusions.

Scenario 3

This scenario considers the source rock potential of both the Lower Vulcan Formation (including its south-western area, although the source rock properties in terms of TOC and HI are here reduced), as well as the Plover source rock interval. *Table 8* compares the fluid properties of the modelled hydrocarbon accumulations to the ones reported in Edwards et al. (2004).

The differentiation of Vulcan and Plover products within an individual accumulation allows the assessment of the respective contribution of these sources:

- Vulcan Formation products: usual 4-compound definition, i.e. Methane, C2-C5, PK_C6-C14 and PK_C15+
- Plover Formation products: characterized by the suffix Pl_, i.e. Pl_Methane, Pl_C2-C5, etc.

Table 8 Field data (Edwards et al., 2004) and the modelled results

	Edwards et al. (2004)				Scenario_3			
Well/Field	**°API**	**GOR (stb/scf)**	**Inferred source rock**	**HC Type**	**°API**	**GOR (stb/scf)**	**SR**	**HC Type**
Leeuwin-1	?	?	?	gas	-	-	-	No accum.
Swan-1,3	40-55	?	L.+U. Vulcan?	gas	42	103000	LV	gas
Tahbilk-1	?	?	L. Vulcan+Plover ?	g/c	23	679	LV	g/c
Cassini-1	40	250	L. Vulcan	g/o	26	471	mixed	oil
Skua-2,3,4,5,8,9	?	700-2000	L. Vulcan	g/o	37 50	1346 21000	LV	gas & oil
Birch-1ST1	43	222	L. Vulcan	oil	25	14200	LV	gas & oil
Challis-1,3,7,8	40	326	L. Vulcan	oil	55	911	LV	traces
Eclipse-2	30-49	?	L. Vulcan	g/o	53	42300	LV	gas & oil
Jabiru-1A,8A,11	42.5	260-350	L. Vulcan	oil	27/55	875/90000	LV	oil & gas
Octavius-1	37.5		L. Vulcan	oil	-	-	-	No accum.
Talbot-1,2	50		L. Vulcan	oil	23	636	LV	oil
Tenacious-1	49	520	L. Vulcan	oil	-	-	-	No accum.
Audacious-1	55	264	L. Vulcan	oil	28	1087	LV	oil/gas
Puffin-1,2,3,5	45	105-197	L. Vulcan +?	oil	18	831	mixed	oil/gas
Pengana-1	45	?	L. Vulcan +?	g/c	26	870	LV	oil
Oliver-1	31.8	628	L. Vulcan + Plover?	g/o	-	-	-	No accum.
Montara-1, 2	34.6	324	Plover?	g/o	23	668	LV	oil
Padthaway-1	34.6	3613	Plover?	g/c	23	668	LV	oil
Crux-1	53.7	?	Plover?	g/c	-	-	-	No accum.
Maple-1	?	?	Plover?	g/o	27	1897	LV	Oil/gas
Bilyara-1 ST1	37	976	Plover?	oil	23	668	LV	oil
Maret-1	39.7	?	Plover coal	condensate	-	-	-	No accum.

Table 9 Fluid compositions (mass fractions, %), calculated by PetroFlash.

	Audacious	Swan 1	Cassini 1	Tahbilk-1	Skua 1	Birch 1	Eclipse 1	Jabiru (oil)	Talbot	Puffin	Pengana 1	Padthaway 1	Maple 1
Methane	19.8	82.8	4.4	5.3	13.6	55.9	75.8	7.7	5.1	4.4	7.7	5.3	16.2
C2-C5	10.7	11.0	6.0	9.2	6.7	11.5	11.7	8.7	9.4	3.0	8.6	9.3	10.0
PK_C6-C14	31.8	4.6	39.2	33.0	50.6	13.3	10.9	38.4	33.9	12.6	38.4	33.3	35.7
PK_C15+	27.3	0.1	36.4	49.4	19.3	14.5	0.0	42.0	51.5	15.9	42.0	50.2	36.4
Pl_Methane	0.7	0.0	0.0	0.1	0.0	0.3	0.0	0.0	0.0	2.5	0.0	0.1	0.0
Pl_C2-C5	1.0	0.0	0.0	0.3	0.1	0.4	0.1	0.2	0.0	5.3	0.2	0.2	0.1
Pl_PK_C6+	3.9	0.2	2.6	1.2	3.1	2.0	1.3	1.3	0.1	24.3	1.3	0.8	0.6
Pl_PK_C15+	4.8	1.3	11.3	1.5	6.5	2.1	0.2	1.7	0.1	31.9	1.7	1.0	0.9
Sum	100	100	100	100	100	100	100	100	100	100	100	100	100

Table 9 shows the contributions of the different source rock units for the wells which were subject in the study of Edwards et al. (2004). From those wells, the Puffin well shows a dominance of Plover generation products (~mol 70%). The gas phase encountered in Jabiru 1 is primarily Vulcan-sourced. Additional accumulations which are also partly sourced by the Plover source rock are modelled for the Langhorne well (Plover ~mol 35%) and Nome well (~mol 20%) and west of Skua and Swift (all in the Puffin Formation reservoir, *Figure 18*). No Plover-sourced accumulation is modelled for Oliver or Maret.

The Eclipse gas/oil accumulation is, on the other hand, sourced to over 95 % by the Vulcan Formation. The Talbot field in the model received petroleum from the Vulcan Formation exclusively. In addition to the petroleum accumulations predicted in Scenario_1, further accumulations were modelled west of Montara (Padthaway 1, location is obscured by well labels) and south of Tahbilk 1 (*Figure 17*). Those oils were sourced from the poor quality Vulcan source rock, which has been assigned to the south-western area.

Figure 19 shows the predicted transformation ratio evolution through time for the Plover source rock unit in the south-western area (location is shown in *Figure 16*). 50% TR was reached in the early Miocene. Organic matter is presently up to 55% transformed. First expulsion occurred at 60 Ma. The onset of petroleum generation occurred in the Early Cretaceous, at 140 Ma. Subsequent generation occurred during a second phase during the Late Oligocene.

Figure 20 shows the predicted transformation ratio evolution through time for the Lower Vulcan source rock unit in the south-western area (location is shown in *Figure 16*). 50% TR has not been reached yet (presently 40% TR). First expulsion occurred at 60 Ma. The onset of petroleum generation occurred at 50 Ma, followed by a sharp drop during the Miocene, and subsequent generation during a second phase during the last 5 Ma.

Results in terms of cumulative hydrocarbon volumes as reported for the Petroleum Systems are shown in the Appendix. The data is available in digital format in the PetroReport module of this scenario. *Figure 21* summarizes the total cumulative volumes of hydrocarbons which were generated, expelled and accumulated. Here it should be taken into account that unexpelled petroleum as well as residual petroleum saturations are included in the “accumu-

lated" volumes. Additionally, due to an error in the PetroReport extraction routine "expelled volumes" are incorrect. This data could, however, not be removed from the graphics as a user-defined output graphic is not available for this option in PetroMod.

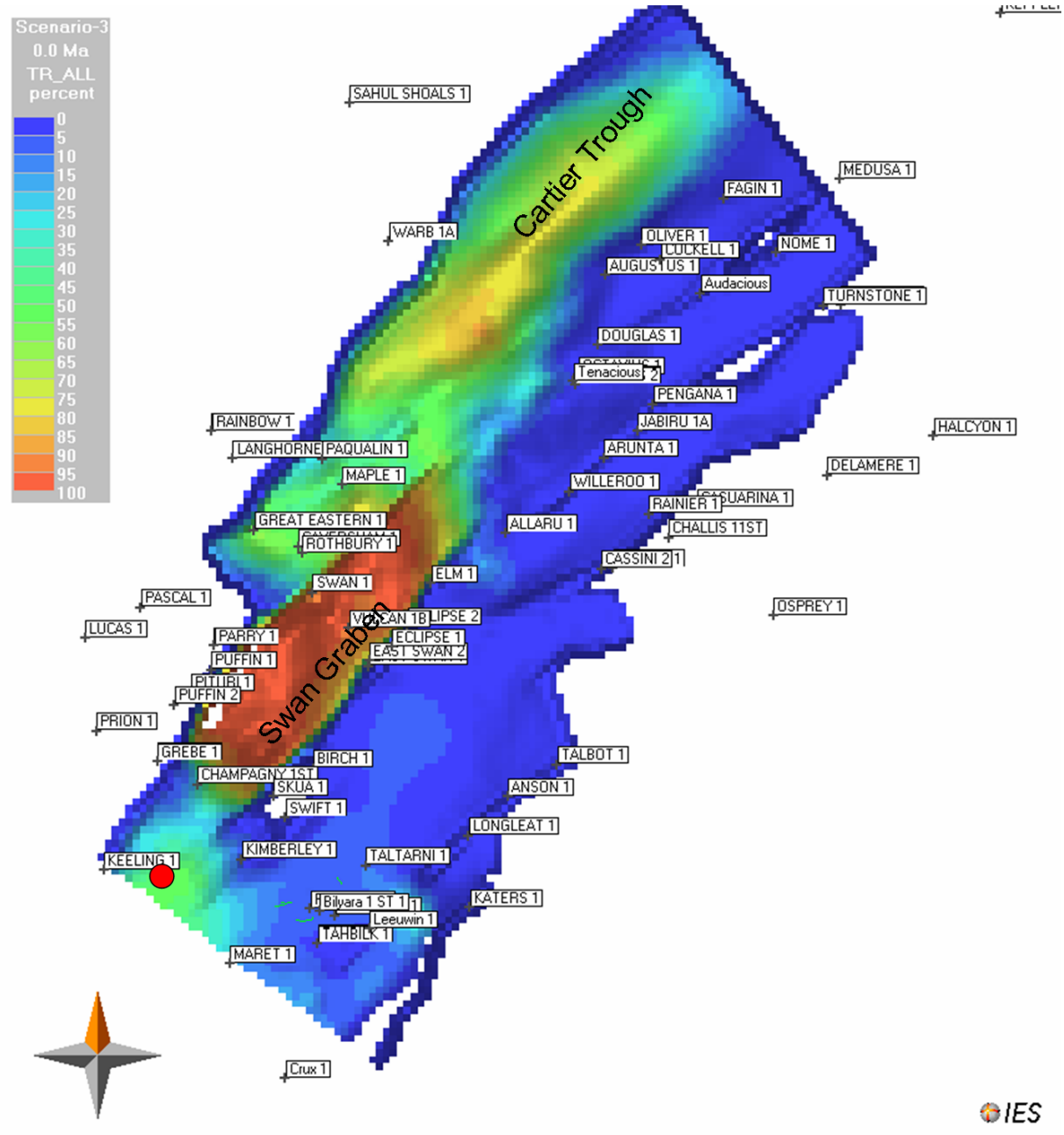

Figure 16 Present Plover source interval. Colour overlay is transformation ratio. The red dot shows the location of the 1D time plot shown in Figure 19.

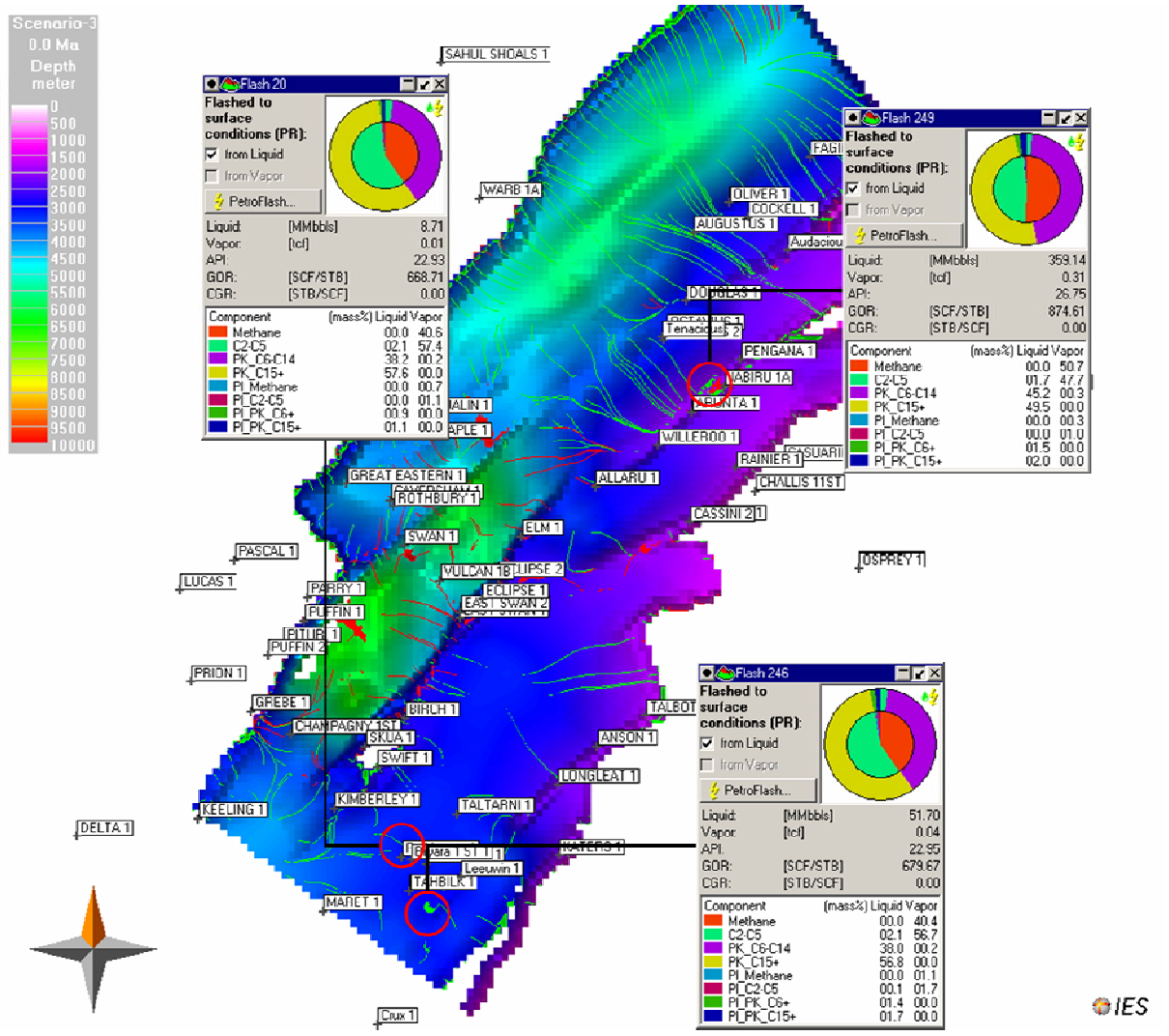

Figure 17 Oil and gas accumulations and flow paths (green/red) in the uppermost Plover Sand_1 (present day, colour overlay is depth). The pie diagrams show the compositions of the Jaribu, Tahbilk and Padthaway accumulations.

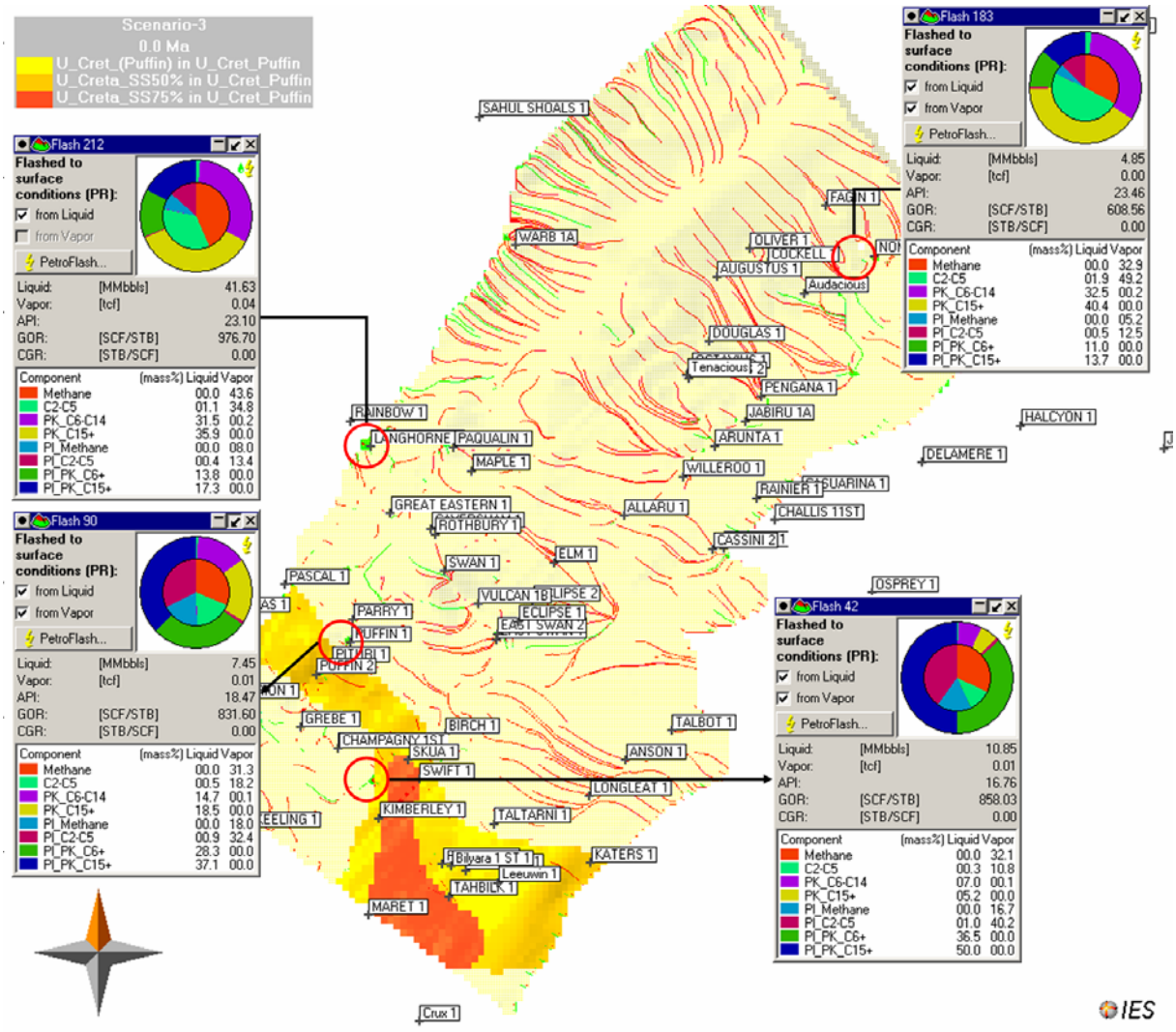

Figure 18 U_Cret. Puffin Formation, present day: Oil (green) and gas (red) accumulations and flow. The pie diagrams show the compositions of the Puffin, Longhorne, Nome accumulations, and an accumulation west of Skua and Swift. Colour overly was switched to transparent, as the accumulations were not clearly visible in the opaque colour mode.

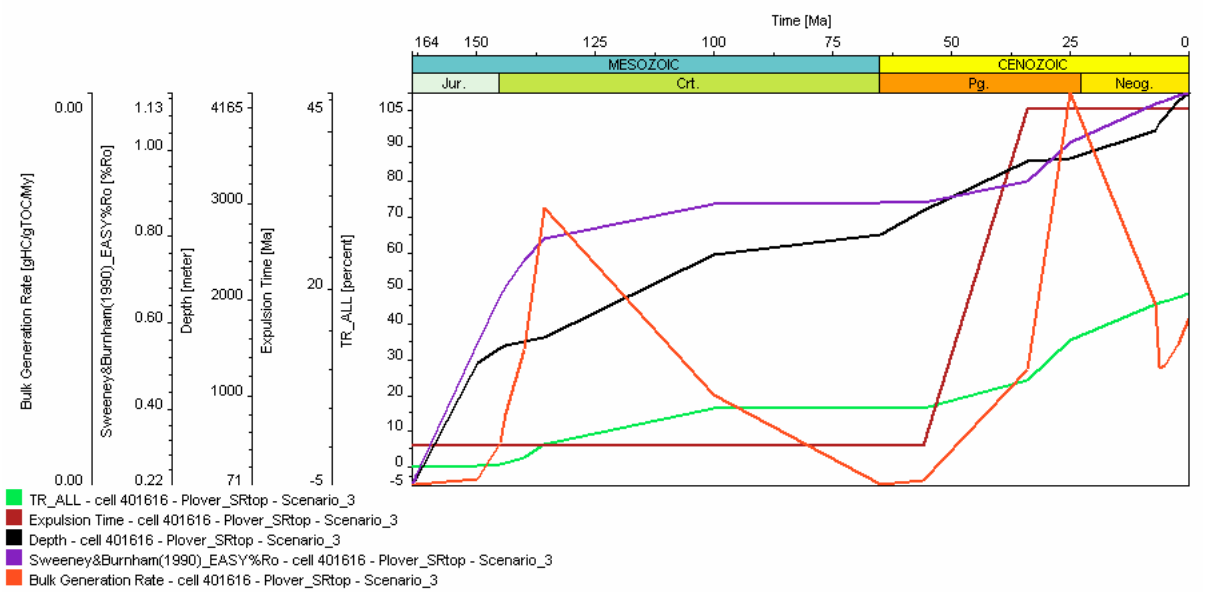

Figure 19 Plover Formation, south-western area: Timing of petroleum generation and expulsion. The 1d time shot location is shown in Figure 16.

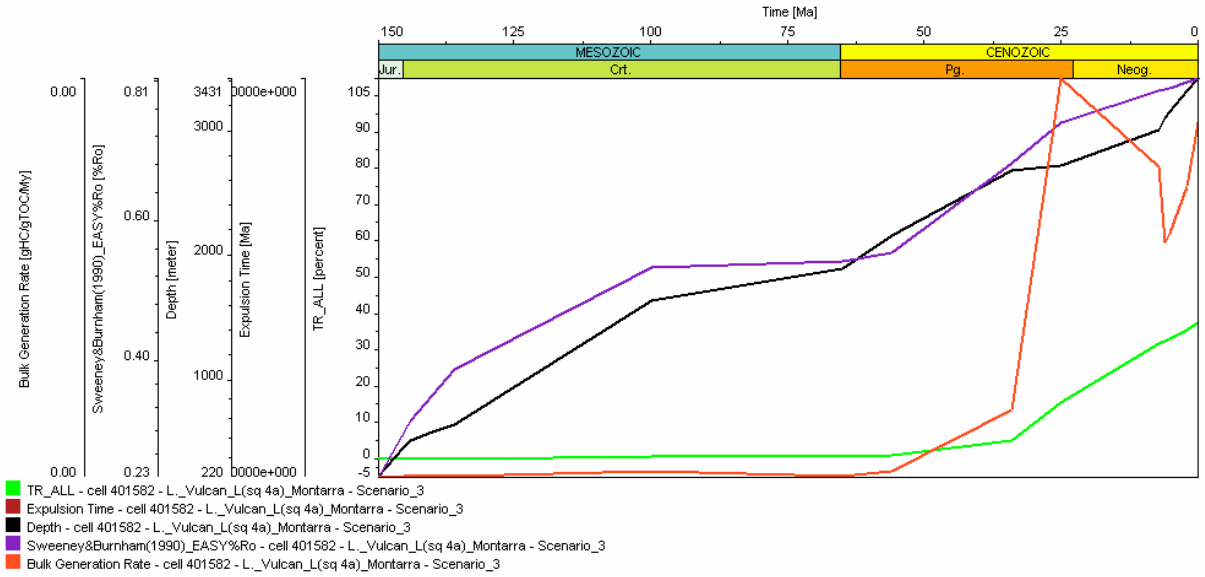

Figure 20 Lower Vulcan Formation, south-western area: Timing of petroleum generation and expulsion. The 1d time shot location is shown in Figure 10.

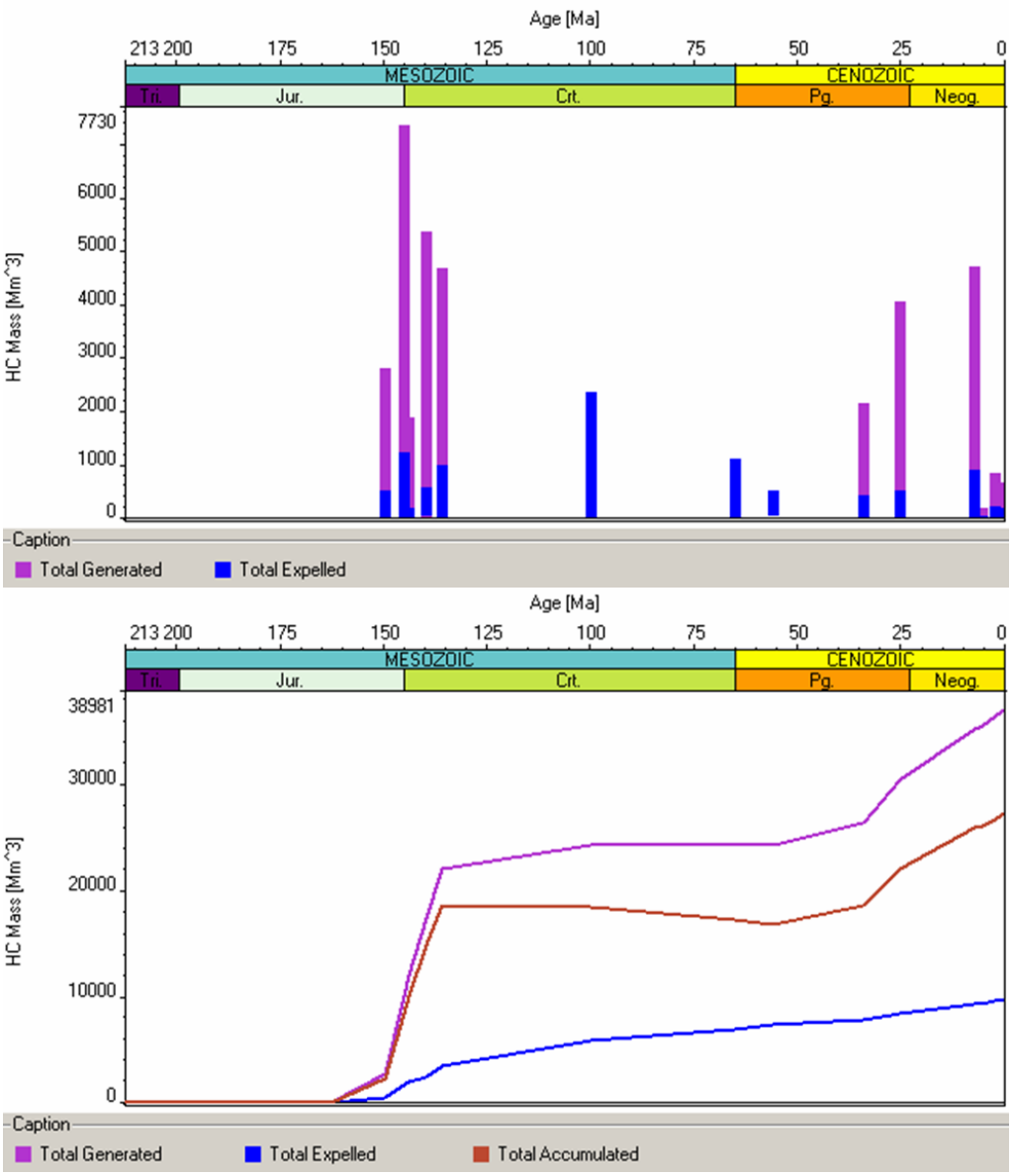

Figure 21 Overview of timing and total volumes of the generated, expelled and accumulated hydrocarbons over time for the entire digital model. Please note that only the generated volumes described here are reliable as discussed in the summary and conclusions.

Scenario 4

This scenario considers the source rock potential of both the Lower Vulcan Formation (including its south-western area) as well as the Plover source rock interval. A lower capillary entry pressure for the sealing Lower Cretaceous formation (see Figure 4) was assigned in order to create a leaky seal. Table 10 compares the fluid properties of the modelled hydrocarbon accumulations to the ones reported in Edwards et al. (2004), and Table 11 shows the contributions of the different source rock units for the wells which were subject in the study of Edwards et al. (2004). From those wells, the Puffin well shows a dominance of Plover generation products (~mol 70%).

Table 10 Field data (Edwards et al., 2004) and the modelled results

	Edwards et al. (2004)				Scenario_4			
Well/Field	**°API**	**GOR (stb/scf)**	**Inferred source rock**	**HC Type**	**°API**	**GOR (stb/scf)**	**SR**	**HC Type**
Leeuwin-1	?	?	?	gas	-	-	-	No accum.
Swan-1,3	40-55	?	L.+U. Vulcan?	gas	40	112000	LV	gas
Tahbilk-1	?	?	L. Vulcan+Plover?	g/c	23	678	LV	g/c
Cassini-1	40	250	L. Vulcan	g/o	24	440	LV	oil
Skua-2,3,4,5,8,9	?	700-2000	L. Vulcan	g/o	35 48	1254 19000	LV	gas & oil
Birch-1ST1	43	222	L. Vulcan	oil	22	13800	LV	gas & oil
Challis-1,3,7,8	40	326	L. Vulcan	oil	49	926	LV	traces
Eclipse-2	30-49	?	L. Vulcan	g/o	52	45000	LV	gas & oil
Jabiru-1A,8A,11	42.5	260-350	L. Vulcan	oil	27/55	872/94000	LV	oil & gas
Octavius-1	37.5		L. Vulcan	oil	-	-	-	No accum.
Talbot-1,2	50		L. Vulcan	oil	23	633	LV	oil
Tenacious-1	49	520	L. Vulcan	oil	-	-	-	No accum.
Audacious-1	55	264	L. Vulcan	oil	28	1089	mixed	oil/gas
Puffin-1,2,3,5	45	105-197	L. Vulcan +?	oil	18	830	mixed	oil/gas
Pengana-1	45	?	L. Vulcan +?	g/c	31	288	LV	oil
Oliver-1	31.8	628	L. Vulcan + Plover?	g/o	-	-	-	No accum.
Montara-1, 2	34.6	324	Plover?	g/o	23	662	LV	oil
Padthaway-1	34.6	3613	Plover?	g/c	23	662	LV	oil
Crux-1	53.7	?	Plover?	g/c	-	-	-	No accum.
Maple-1	?	?	Plover?	g/o	27	1889	LV	oil/gas
Bilyara-1 ST1	37	976	Plover?	oil	23	662	LV	oil
Maret-1	39.7	?	Plover coal	condensate	-	-	-	No accum.

Table 11 Fluid compositions (mass fractions, %), calculated by PetroFlash.

	Audacious 1	Swan 1	Cassini 1	Tahbilk 1	Skua 1	Birch 1	Eclipse 1	Jabiru (oil)	Jabiru 1 (gas)	Talbot	Puffin	Pengana 1	Padthaway 1	Maple 1
Methane	21.0	83.1	4.1	5.3	12.8	55.4	76.3	7.7	74.2	5.0	4.2	2.5	5.2	16.2
C2-C5	10.8	11.1	5.6	9.3	6.4	10.9	11.7	8.6	19.2	9.4	2.7	6.7	9.3	9.8
PK_C6-C14	32.1	4.1	37.0	33.2	50.0	12.0	10.2	38.6	5.6	33.9	11.1	48.8	33.3	35.6
PK_C15+	26.4	0.1	40.1	49.6	21.5	15.4	0.0	41.7	0.0	51.4	13.8	39.1	50.4	36.6
Pl_Methane	0.6	0.0	0.0	0.1	0.0	0.3	0.0	0.0	0.4	0.0	2.8	0.0	0.1	0.0
Pl_C2-C5	1.0	0.0	0.0	0.2	0.1	0.5	0.1	0.2	0.4	0.0	5.6	0.2	0.2	0.1
Pl_PK_C6+	3.7	0.2	2.3	1.0	2.6	2.3	1.4	1.3	0.2	0.1	25.9	1.1	0.7	0.6
Pl_PK_C15+	4.4	1.3	10.9	1.3	6.5	3.2	0.2	1.8	0.0	0.1	34.0	1.6	0.9	1.0
Sum	100.0	100	100	100	100	100	100	100	100	100	100	100	100	100

Results in terms of cumulative hydrocarbon volumes as reported for the Petroleum Systems are shown in the Appendix. The data is available in digital format in the PetroReport module of this scenario. *Figure 24* summarizes the total cumulative volumes of hydrocarbons which were generated, expelled and accumulated. Here it should be taken into account that un-expelled petroleum as well as residual petroleum saturations are included in the “accumulated” volumes. Additionally, due to an error in the PetroReport extraction routine “expelled volumes” are incorrect. This data could, however, not be removed from the graphics as a user-defined output graphic is not available for this option in PetroMod.

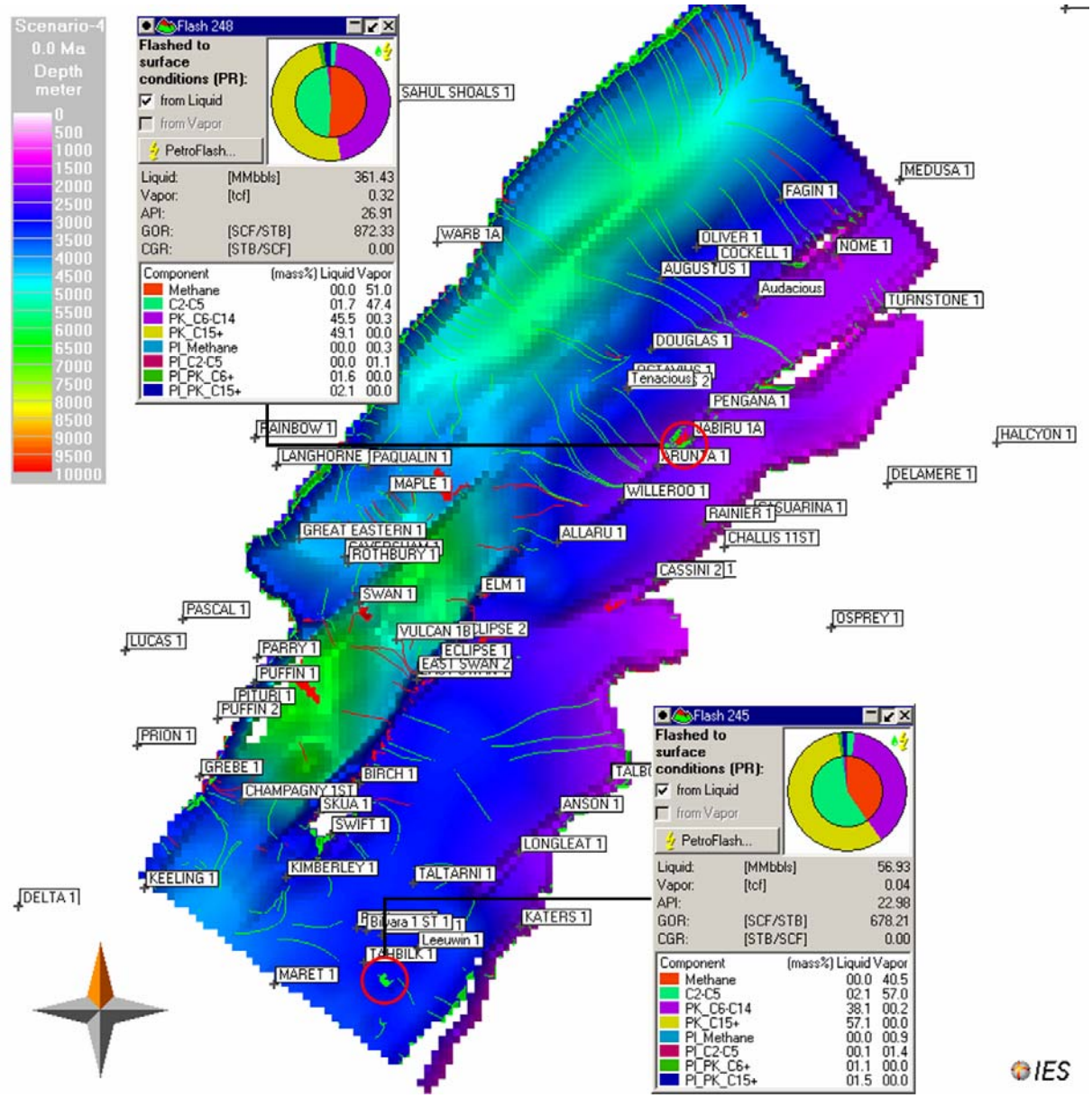

Figure 22 Oil and gas accumulations and flow paths (green/red) in the uppermost Plover Sand_1 (present day, colour overlay is depth). The pie diagrams show the compositions of Jabiru 1A and Tahbilik 1 accumulations.

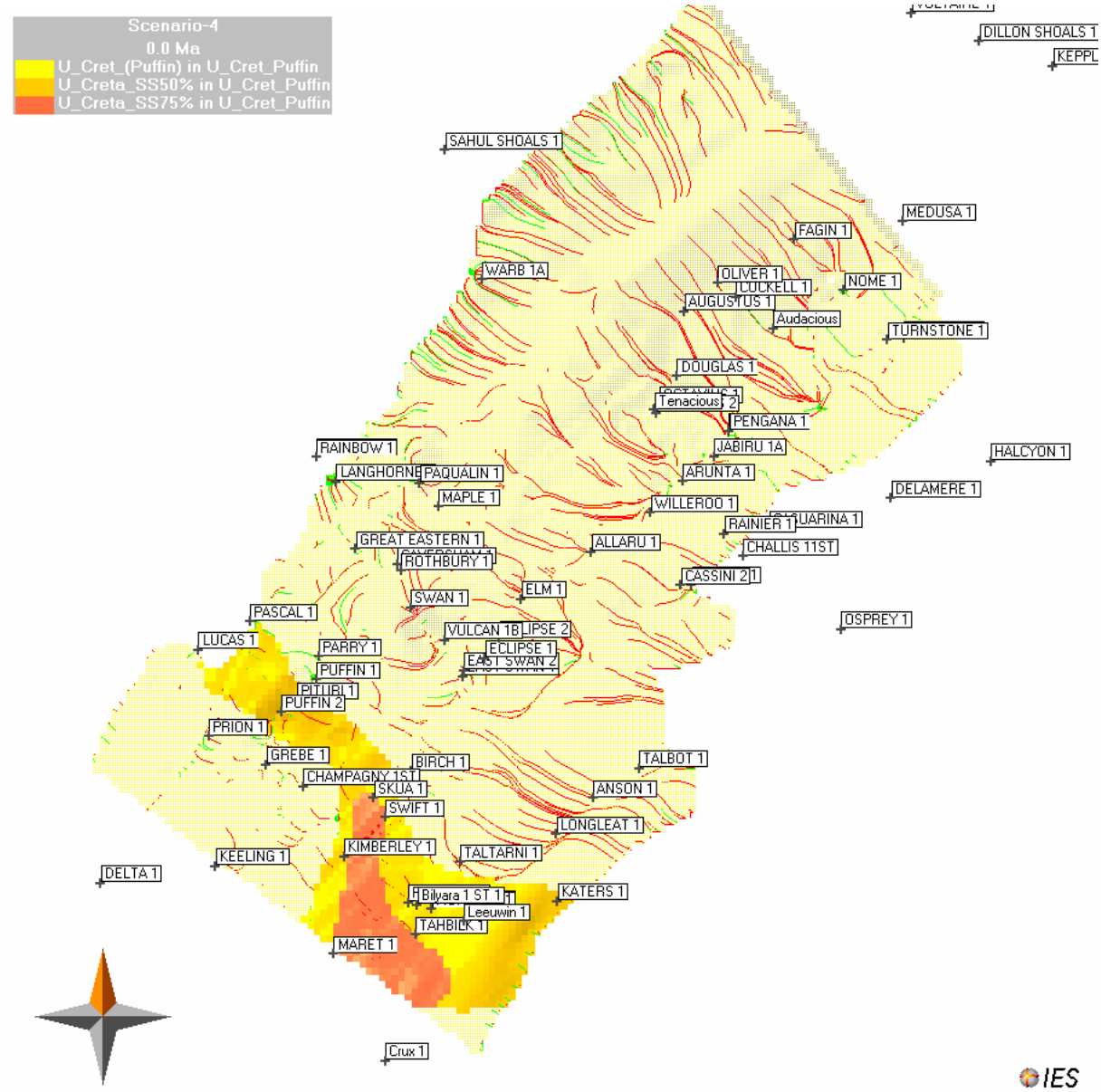

Figure 23 U_Cret. Puffin Formation, present day: Oil (green) and gas (red) accumulations and flow.

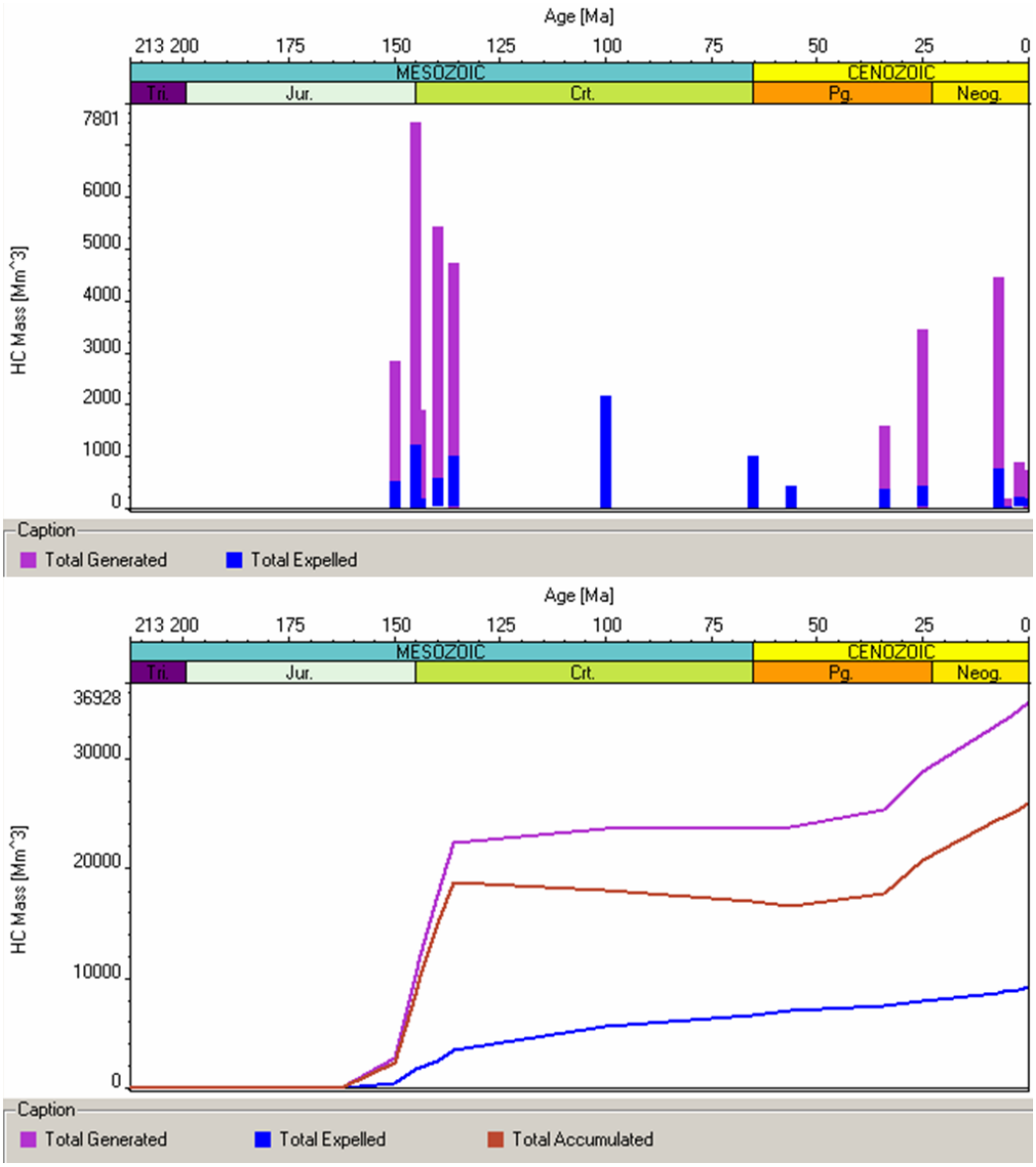

Figure 24 Overview of timing and total volumes of the generated, expelled and accumulated hydrocarbons over time for the entire digital model. Please note that only the generated volumes described here are reliable as discussed in the summary and conclusions.

Scenario 5

This scenario tested hydrocarbon charge along faults during rifting episodes. Both Plover and Lower Vulcan (including its south-western area) are assigned as source rocks.

As in the former scenarios, Vulcan and Plover products were tagged in order to allow a differentiation of the generated products:

- Vulcan Formation products: usual 4-compound definition, i.e. Methane, C2-C5, PK_C6-C14 and PK_C15+
- Plover Formation products: characterized by the suffix Pl_, i.e. Pl_Methane, Pl_C2-C5, etc.

The fault distribution is shown in Figure 26. Table 12 compares the fluid properties of the modelled hydrocarbon accumulations to the ones reported in Edwards et al. (2004).

The contributions of the different source rock units (Table 13) show that the accumulation modelled for the area of Puffin has a dominance of Plover generation products (~mol 65%), together with additional accumulations around the Puffin well. The rest of the modelled area shows only minor contributions of Plover generation products of up to ~mol 10%. The fluid composition of the modelled hydrocarbon accumulations is very similar to the ones modelled in Scenario 3.

A very small oil accumulation of about 0.8MMbbls is trapped (exclusively in this scenario) at the faults at Octavius 1. No accumulation was modelled for Audacious, as the modelled oil is trapped on the western side of fault west of the well (Figure 25).

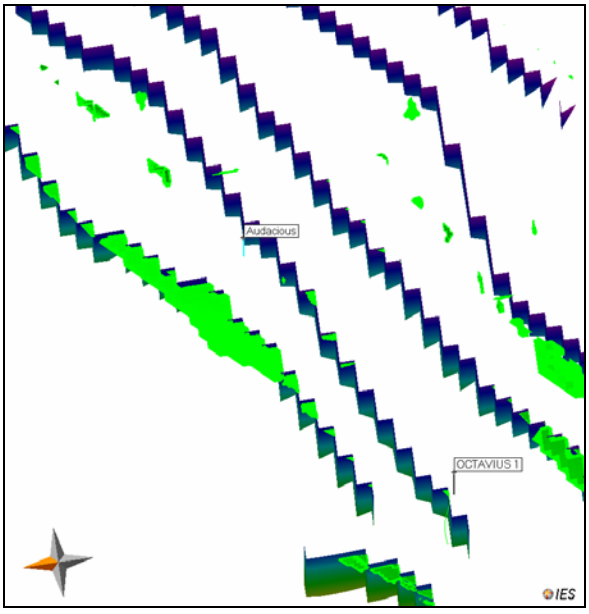

Figure 25 Rotated view on fault pattern an d accumulations at the two wells.

The assigned fault properties resulted in a general reduction of both Vulcan and Plover generation products in the accumulations encountered within the Vulcan Sub-basin (e.g. Jabiru here: 185MMbbls, 365MMbbls in scenario 3). Such Plover products are restricted to very specific areas around Puffin. In general, the introduction of the faults in this scenario lead to larger hydrocarbon accumulations in many areas throughout the basin, e.g. at Maple, Douglas and Swift/Skua, as hydrocarbon migration is hindered in those areas by the faults. As a

result the accumulations are comparably larger at those sites. However, other areas do not show significant influence on either the distribution or size of HC accumulations.

Figure 27 summarizes the total cumulative volumes of hydrocarbons which were generated, expelled and accumulated. Here it should be taken into account that un-expelled petroleum as well as residual petroleum saturations are included in the "accumulated" volumes. Additionally, due to an error in the PetroReport extraction routine "expelled volumes" are incorrect. This data could, however, not be removed from the graphics as a user-defined output graphic is not available for this option in PetroMod.

Table 12 Vulcan Sub-basin source-related petroleum groups (Edwards et al., 2004) and the modelled results.

	Edwards et al. (2004)				Scenario_5			
Well/Field	**°API**	**GOR (stb/scf)**	**Inferred source rock**	**HC Type**	**°API**	**GOR (stb/scf)**	**SR**	**HC Type**
Leeuwin-1	?	?	?	gas	-	-	-	No accum.
Swan-1,3	40-55	?	L.+U. Vulcan?	gas	28	400000	LV	g/o
Tahbilk-1	?	?	L. Vulcan + Plover?	g/c	23	684	LV	g/c
Cassini-1	40	250	L. Vulcan	g/o	33	585	LV	oil
Skua-2,3,4,5,8,9	?	700-2000	L. Vulcan	g/o	27	2135	LV	g/o
Birch-1ST1	43	222	L. Vulcan	oil	47	40000	LV	g/o
Challis-1,3,7,8	40	326	L. Vulcan	oil	37	813	LV	traces
Eclipse-2	30-49	?	L. Vulcan	g/o	51	30000	LV	g/o
Jabiru-1A,8A,11	42.5	260-350	L. Vulcan	oil	30	832	LV	g/o
Octavius-1	37.5		L. Vulcan	oil	23	763	LV	oil
Talbot-1,2	50		L. Vulcan	oil	23	638	LV	oil
Tenacious-1	49	520	L. Vulcan	oil	-	-	-	No accum.
Audacious-1	55	264	L. Vulcan	oil	-	-	-	No accum.
Puffin-1,2,3,5	45	105-197	L. Vulcan +?	oil	19	811	L. Vulcan + Plover	g/o
Pengana-1	45	?	L. Vulcan +?	g/c	30	827	LV	oil
Oliver-1	31.8	628	L. Vulcan + Plover?	g/o	-	-	-	No accum.
Montara-1, 2	34.6	324	Plover?	g/o	23	656	LV	oil
Padthaway-1	34.6	3613	Plover?	g/c	23	660	LV	oil
Crux-1	53.7	?	Plover?	g/c	-	-	-	No accum.
Maple-1	?	?	Plover?	g/o	30	2068	LV	g/o
Bilyara-1 ST1	37	976	Plover?	oil	-	-	-	No. Accum.
Maret-1	39.7	?	Plover coal	condensate	-	-	-	No accum.

Table 13 Fluid compositions (mass fractions, %), calculated with PetroFlash.

	Swan 1	Cassini 1	Tahbilk-1	Skua 1	Birch 1	Eclipse 1	Jabiru 1	Talbot	Puffin	Pengana 1	Padthaway 1	Maple 1
Methane	85.0	5.1	5.4	18.9	69.0	69.1	8.0	5.1	5.5	8.0	5.2	17.0
C2-C5	12.2	9.1	9.3	7.4	16.4	13.7	7.2	9.4	3.4	7.2	9.4	11.3
PK_C6-C14	1.8	49.5	33.2	33.8	9.5	13.0	44.4	33.9	14.3	44.5	33.6	37.0
PK_C15+	0.1	35.7	49.7	28.6	0.3	0.2	35.0	51.6	12.4	34.9	51.0	31.4
Pl_Methane	0.0	0.0	0.1	0.1	0.8	0.2	0.0	0.0	1.6	0.0	0.0	0.2
Pl_C2-C5	0.1	0.0	0.2	0.4	0.9	0.8	0.2	0.0	4.1	0.2	0.1	0.3
Pl_PK_C6+	0.2	0.1	0.9	4.3	2.2	3.0	2.4	0.0	24.8	2.4	0.3	1.2
Pl_PK_C15+	0.6	0.3	1.2	6.4	0.9	0.1	2.9	0.0	34.0	2.9	0.4	1.5
Sum	100	100	100	100	100	100	100	100	100	100	100	100

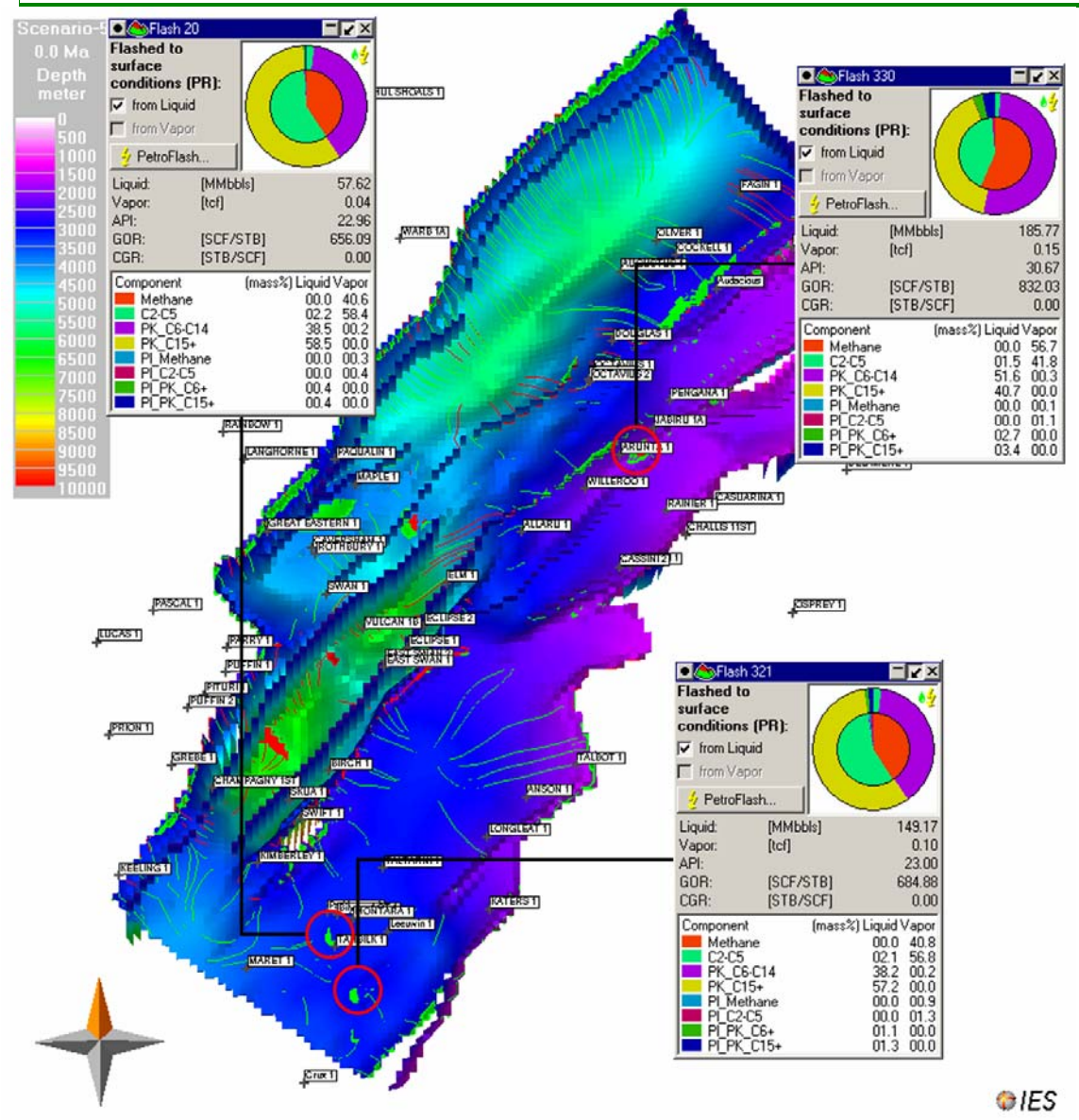

Figure 26 Fault distribution, oil and gas accumulations and flow paths (green/red) in the uppermost Plover Sand_1 (present day, colour overlay is depth). The pie diagrams show the compositions of the Jaribu, Tahbilk and Padthaway 1 accumulations.

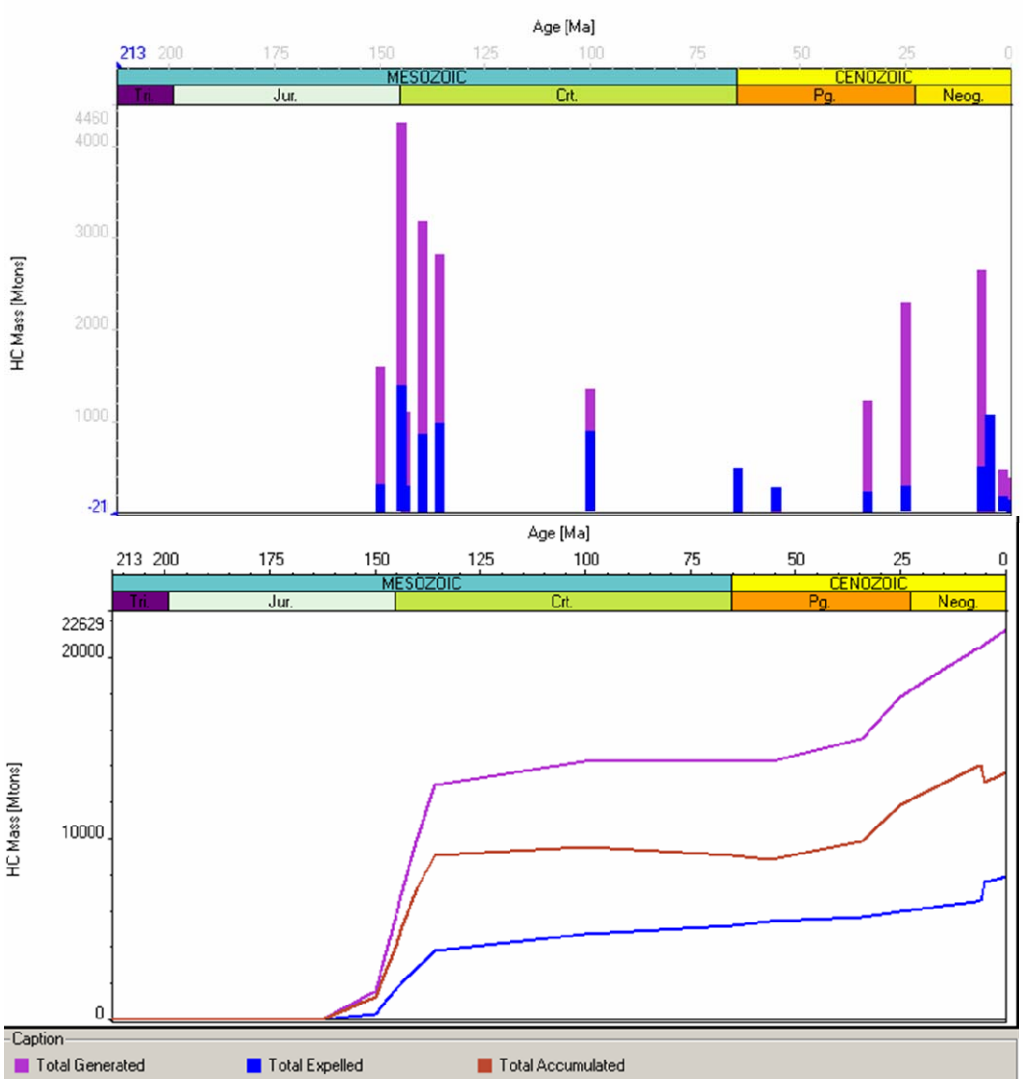

Figure 27 Overview of timing and total volumes of the generated, expelled and accumulated hydrocarbons over time for the entire digital model. Please note that only the generated volumes described here are reliable as discussed in the summary and conclusions.

Summary and Conclusions

Several scenarios of an original 3D model based on the petroleum systems model of Fujii et al. (2004) were simulated using the PetroMod™ 3D V.10 modeling software.

In general the results of the modelling study presented here confirms the modelling results of Fujii et al. (2004) with respect to the timing of generation in the different sub-basins as well as present day maturity. The main differences between the work of Fujii et al. (2004) and the work presented here are based on the use of PhaseKinetic models for the individual source rock formations and the ensuing compositional predictions of the fluids in different fields.

Source rock transformation ratios as well as the bulk generation rates indicate that the source rocks are presently still generating. The Central Swan Graben area is presently more mature than the other kitchen area of the Vulcan Sub-basin, the Cartier Trough.

Within the Swan Graben, the main phase of petroleum generation and migration occurred for all scenarios between the upper Late Jurassic to the Early Cretaceous. Within the Cartier Trough, generation/migration occurred later, in the middle and late Tertiary. The modelling results suggest that both reservoir and sealing units were sufficiently developed to retain even the initial charge. The Vulcan source rock shows an increase in the degree of kerogen transformation during the Neogene burial up to the present day indicating currently ongoing petroleum generation.

Predictions regarding the timing of main hydrocarbon generation match those reported by Fujii et al. (2004) closely, indicating that the kinetic models used in both cases were also grossly similar.

The locations of predicted accumulations coincide with the locations of most of the proven fields. In many cases accumulation sizes and predicted column heights are large, mainly due to the fact that the resolution of the numerical model is low which leaves rather large volumes of the cells to be filled.

Modelling results predict a series of accumulations at locations which have, as yet, not been tested. However, most of them depend on fault closure, thus increasing exploration risk.

The main risks as observed from this modelling exercise are

- source rock presence and definition,
- definition of the traps,
- resolution of the input model,
- cap rock properties, which are still largely unconstrained.

The different scenarios modelled show distinct variations with respect to predicted petroleum distribution as well as the physical properties of the accumulated fluids. Interestingly Scenarios 1 and 2, where only the Vulcan Formation was defined as a source rock, show the highest GORs. Scenarios 3, 4 and 5 which included the Plover Formation show a predominance of accumulations with lower GORs which better match the natural fluid compositions. The reduced gas-proneness of the Plover models indicates that fluids generated by the

deeper source rock probably facilitate expulsion and increase migration efficiency from the Vulcan source rock in the model. This effect is due to the early saturation of migration pathways with hydrocarbons, reducing thus the losses of Vulcan-generated fluids in the form of residual petroleum saturation. As expulsion from the source rock in the model is controlled by kerogen conversion, adsorption and pressure gradients within the source rock release of fluids occurs both in an upward and downward direction. In view of the relatively impermeable formations overlying the Vulcan source the bulk of generated hydrocarbons is expelled into the underlying Plover carrier system, as also indicated by Fujii et al. (2004). If an active Plover source rock contributes fluids from below into the same carrier system obviously the migration pathways would be saturated by this early charge first, paving the way for later Vulcan sourced fluids.

The general observation that GORs sink when the Plover source rock is included is not valid for all accumulations. A large structural closure east of Maple shows a shift from an oil to an oil-rimmed gas accumulation in going from Scenarios 1 and 2 to Scenarios 3, 4 and 5. Here it appears likely that the slight increase in total generated volumes affects the phase state in a given accumulation. As discussed above, the early saturation of migration pathways by Plover products would increase migration efficiency of Vulcan products resulting in earlier migration and accumulation of low maturity petroleum. In the course of simulated time in the model this would lead to a shift in the maturity of migrating fluids between the two Scenario types (with Plover and without), where in the Vulcan–only case a slightly higher maturity of migrating fluids at any timestep would be expected as compared to slightly lower maturities where both source rocks are included. Depending then on whether a reservoir traps the cumulative products generated or an instantaneous phase (only a portion of the total migrating fluid) then drastic differences in the reservoir fluid composition can be expected. Identifying the exact process leading to the definition of the fluid type trapped in a specific trap in a basin model is, however, due to the complexity of the models extremely difficult.

Due to errors identified in the PetroReport data extraction routine a complete mass balance of volumes of petroleum generated, expelled and accumulated could not be performed. As corroborated by IES, when secondary cracking is taken into account the extraction routines fail to correctly address expelled and accumulated volumes. Generated volumes, however, are correct as can be seen from the comparison of generated and accumulated volumes of all Scenarios where differences are only minor. The calculation of the “accumulation efficiency” of the individual scenarios run, which is the percentage of oil accumulated in the Puffin and Plover reservoirs as a function of the total generated, results in values below 2% for Scenarios 1 to 4 and 2.9% for Scenario 5 where vertical permeable faults were taken into account. Here it should be noted, that variations in the generated volumes up to around 10-15% do not imply a drastically different geologic history. Due to the forward modelling approach used in PetroMod every simulation is unique and a perfect reproduction of earlier results of e.g. the same simulation is not actually possible. Due to the continuous correction of sediment deposition rates to decrease the difference between input tops and calculated tops (the so called “optimisation” procedure in PetroMod) slight differences in sediment thicknesses occur between different simulations resulting in slightly different calculation results with respect to e.g. the amount of hydrocarbons generated.

According to IES the error found in the PetroReport data extraction routines is due to the complexity of tracking cracking products from different sources as well as the occurrence of

cracking both within the source as well as outside of it. It appears unlikely that this error in PetroMod will be repaired as part of Version 10 patches, or even within Version 11. The error, however, seems to lie within the data extraction tool and not in the simulation itself. Accordingly we expect that the results available in the 3D PetroMod viewer are correct and only data extractions of expelled volumes by PetroReport are in error.

Secondary migration as modelled in the study area is dominantly controlled by capillary failure of the seals at structural closures or stratigraphic pinch outs. Versions of the model run taking variable fault properties into account did not result in significant changes in hydrocarbon distribution. Even in Scenario 5, where vertical, temporarily permeable faults were implemented no significant increase in accumulation efficiency was monitored (increase from an average of around 2% to 2.9% in Scenario 5). These results are an artefact of the migration method used. The Hybrid migration method of PetroMod, where the sedimentary sequence is subdivided into carriers and non-carriers based on a permeability threshold, uses different methods for the calculation of migration in carriers and non-carriers. In non-carriers migration is calculated assuming Darcy flow. Accordingly permeability, saturation, viscosity and time are taken into account. In carriers a ray tracing approach is applied, where migration is instantaneous within the carrier and all fluids in a carrier are moved to the structurally highest position forming an accumulation or leaking into the next sedimentary unit. In the implementation of vertical faults as conduits of migration the applied Hybrid migration method hence would only lead to significant vertical flow of hydrocarbons along a fault if an accumulation is present in contact with the fault. Otherwise the instantaneous movement of fluids in the carrier to the highest position largely bypasses the faults.

Model resolution and the degree of geologic simplification are the main reasons for the observed controls on migration processes. As discussed earlier, homogeneous sedimentary facies are assumed for most of the stratigraphic units. In combination with continuous layers as defined by the maps provided this results in a relatively clear “layer cake” model in which sedimentary pinch-outs, facies changes and faults play a very subordinate role. Accordingly capillary entry pressure is the main leakage mechanism modelled, simply because more complex geologic situations could not be included in the model. Regarding the interpretation of Kivior et al. (2002), where top seal capillary failure was not seen as the main mechanism for trap failure, it must be taken into account that the implementation of seal capacity measurements into a regional model such as the one presented here is complex due to upscaling requirements from lab scale to regional scale as well as the implicit assumption that the measurement made is actually correct for the entire cap rock. Both subjects are the topics of intense discussion both in basin modelling and reservoir engineering circles.

Where terminations were included large stratigraphic accumulations are modelled, e.g. along the western flank of the Swan Graben within the Plover sand, which is here assumed to be juxtaposed to the older non-permeable strata along the main boundary fault. The Lower Cretaceous and Vulcan units provide the cap rocks for these accumulations. While the validity of this trap type has not been tested in the area it could be indicative of a potential new play, especially in view of the fact that most of the Cretaceous accumulations west of the main boundary fault depend on focussing of migration along the flanks of the basin and vertical leakage into the Cretaceous carrier.

Significant variations in predicted versus observed fluid API gravities are due to the lack of predictive capacity of the compositional kinetic models used. In general even PhaseKinetic models are not API predictive, as the physical properties of the liquid pseudo-components

are identical for all source rock models used. Accordingly these models predict a realistic, albeit, limited range of API gravities (usually extending from roughly 30° API during primary cracking to 50° API when secondary cracking becomes dominant). The 4-compound models used in this study are known to produce too heavy API gravities; however, the phase behaviour of the fluids generated matches that of the PhaseKinetic models (see Appendix 2).

Tagging of the kinetic models for the Vulcan and Plover Formations allowed the recognition of relative contributions of the individual source units to specific accumulations. In most of the accumulations a clear dominance of Vulcan generation products is observed, as is the case for the Eclipse (>95%) or Talbot (100%) accumulations. The Puffin field, however, shows a marked discrepancy in the model: roughly 70% of the oil is modelled to have been generated by the Plover Formation. This is most likely due to the location of a high porosity sandstone defining the drainage area of the Puffin accumulation. This sandstone lies directly above one of the main depocenters of the Swan Graben, and, hence, catches high maturity products migrating in a vertical direction. Edwards et al. (2004) argue in favour of migration up the main boundary fault on the basin margin during fault movement or reactivation. As discussed earlier the use of faults as vertical migration pathways in PetroMod is difficult to implement. Accordingly which mechanism is more likely to be the right one is difficult, or even impossible to test. However, whether the fluids migrate up the fault and into the carrier sand or vertically through the Jurassic and Cretaceous sequences via capillary failure and then into the late Cretaceous carrier system does not make a big difference. Based on the model results, should the natural composition of the Puffin oil indicate a dominant Vulcan source then the Puffin Cretaceous drainage area needs to be revised.

Limitations of the 3D model developed in this study are clearly to be found in the model resolution. A smaller grid size and higher resolution would help in better investigating the evolution of the study area especially with respect to migration and reservoir filling. A prime example is the modelled continuous Eclipse accumulation. In the natural system these reservoirs are most likely a series of fault bounded rotated fault blocks; in the model they consist of softly folded continuous sands. Accordingly individual reservoir compartments can not be modelled and all fluids reaching any of the prospects mix into one single accumulation.

The Tahbilk, Montara, Bilyara and Padthaway fields, as well as the nearby located undrilled structural closures, are other examples of resolution and geologic simplification problems. Structural closures in these location were either extremely subtle or essentially absent in the maps provided, whereas structural closures occur where neighbouring undrilled accumulations are modelled. Definition of a fault bounded trap for these fields was not implemented due to lack of information regarding the actual prospect structures. For the assessment of fluid composition and physical properties the structural closure and accumulation west of the Montara well in the model were assumed to be representative of these fields. In the case of Bilyara no nearby accumulation was modelled and hence the fields could not be included in the assessment of Plover vs. Vulcan contributions.

Fluid occurrence and compositional predictions in the South-Western area of the models were not entirely satisfactory. The predicted main source for the Montara field is the Lower Vulcan Formation in the model, whereas Edwards et al. (2004) identified a likely Plover origin of the hydrocarbons. These modelling results possibly indicate that the assumption of the presence of a Vulcan source rock in the area may be questionable. Additionally, the possible contribution from a kitchen area outside (South East) of the modelled area supplying hydrocarbons to this field, e.g. from the Heywood Graben, should be taken into account.

Edwards et al. (2004) indicated that the Puffin Field although assigned to their Group A (Vulcan sourced) could contain an additional input from the Plover formation. Modelling results indicate a significant Plover contribution as discussed above, attributable to the presence of an Upper Cretaceous sand body which drapes over the Swan Graben and focusses fluids entering vertically from the Graben towards the flanks of the basin where the Puffin structure is located. Here again the predicted fluid compositions are obviously controlled by the geologic assumptions implemented into the model.

This study was performed in order to see whether fluid compositional predictions can be made at a basin scale. In general those models in which both source rocks had been taken into account gave the best results with respect to predicting the overall distribution of oil vs. gas in the study area. A high fluid variability was predicted with the co-occurrence of single phase oil, two phase systems as well as single phase gas accumulations. In general also the regional distribution was reproduced. When it comes to GOR prediction, the modelling results tended to be generally in the ball park, but by far not perfect. Predicted GORs are roughly twice as high as observed, e.g. in Cassini, Challis, Jabiru, Montara and Puffin. Prediction vs. observation of gas and condensate occurrence matched for Swan and Maple. Two phase systems were correctly predicted for East Swan, Eclipse, Maple and Skua. All of these results are based on Scenario 3.

The question whether Plover coals generate and expel liquid hydrocarbons can not be answered conclusively by this study. Based on the compositional kinetic models available, one for each source rock, the Plover source can generate and expel liquids. Plover and Vulcan source rocks do not differ drastically based on the products they generate upon artificial maturation. The question remains whether the samples used for the determination of compositional kinetics are actually representative for the source rocks in the basin, or whether facies and ensuing kinetic variability may play an important role in the Vulcan Sub-Basin.

As compared to their studies regarding compositional predictions on a prospect to basin scale, it has become evident that the larger the scale of the basin, the more difficult it is to correctly reproduce natural GORs. Studies performed at GFZ as part of industry collaborations have shown that accurate GOR predictions are possible when working close to the prospect scale (e.g. di Primio & Neumann, 2008; di Primio & Skeie, 2004). Working at a semi regional to regional scale immediately implies a much lower resolution and therefore a lower GOR predictive capacity. As seen in the present Vulcan Sub-Basin study, predictions regarding fluid type and general GOR are, however, still relatively good offering the explorationist at least a rough assessment of the fluid type to be expected and reducing, thus, exploration risk. For an accurate prediction of petroleum phase and physical properties, however, a much higher resolution of the model is required, in a stratigraphic, facies, temporal and structural sense.

References

Andresen, B., Throndsen, T., Barth, T., Bolstad, J., (1994) Thermal generation of carbon dioxide and organic acids from different source rocks. *Organic Geochemistry*, 21(12), 1229-1242.

Behar, F., Ungerer, P., Kressmann, S., Rudkiewicz, J.L., (1991) Thermal evolution of crude oils in sedimentary basins; experimental simulation in a confined system and kinetic modeling. *Revue de l'Institut Francais du Petrole*, 46(2), 151-181.

Berner, U., Faber, E., Scheeder, G., Panten, D., (1995) Primary cracking of algal and landplant kerogens; kinetic models of isotope variations in methane, ethane and propane, *Processes of natural gas formation*, *126; 3-4*, pp. 233-245. Elsevier, Amsterdam, Netherlands.

Bradshaw, M.T., Bradshaw, J., Murray, A.P., Needham, D.J., Spencer, L., Summons, R.E., Wilmot, J., Winn, S., (1994) Petroleum systems in West Australian basins. *The Sedimentary Basins of Western Australia: Proceedings of Petroleum Exploration Society of Australia Symposium*, 1, 93-118.

Cadman, S.J., Temple, P.R., (2003) Bonaparte Basin, NT, WA, AC & JPDA. In: *Australian Petroleum Accumulations Report 5, 2nd Edition*, pp. 335. Geoscience Australia, Canberra.

Chen, G., Hill, K.C., Hoffmann, N., (2002) 3D structural analysis of hydrocarbon migration in the Vulcan subbasin, Timor Sea. In: *The Sedimentary Basins in Western Australia 3*, *Proceedings in the PESA Symposium, Perth, WA* (Ed. by M. Keep, S.J. Moss), Perth.

di Primio, R., Dieckmann, V., Mills, N., (1998) PVT and phase behaviour analysis in petroleum exploration. *Organic Geochemistry*, 29(1-3), 207-222.

di Primio, R., Horsfield, B., (2004) Development of compositional kinetic models for hydrocarbon generation and phase behaviour modelling. In: *Goldschmidt Conference*, Copenhagen.

di Primio, R., Horsfield, B., (2006) From petroleum type organofacies to hydrocarbon phase prediction. *AAPG Bulletin*, 90(7), 1031-1058.

di Primio, R., Neumann, V., (2008) HPHT reservoir evolution: a case study from Jade and Judy fields, Central Graben, UK North Sea. In: *International Journal of Earth Sciences*, *97* (Ed. by U. Bayer, D. Gajewski, R. Littke), pp. 1101-1114. Springer.

di Primio, R., Skeie, J.E., (2004) Development of a compositional kinetic model for hydrocarbon generation and phase equilibria modelling: a case study from Snorre Field, Norwegian North Sea. In: J.M. Cubitt, England, W. A., Larter, S. (Ed.), *Understanding Petroleum Reservoirs: towards an Intefrated Reservoir Engineering and Geochemical Approach*, *237* (Ed. by J.M. Cubitt, England, W. A., Larter, S.), pp. 157-174. Geological Society, London.

Dieckmann, V., Schenk, H.J., Horsfield, B., Welte, D.H., (1998) Kinetics of petroleum generation and cracking by programmed-temperature closed-system pyrolysis of Toarcian Shales. *Fuel*, 77(1-2), 23-31.

Edwards, D.S., Preston, J.C., Kennard, J.M., Boreham, C.J., van Aarssen, B.G.K., Summons, R.E., Zumberge, J.E., (2004) Geochemical characteristics of hydrocarbons from the Vulcan Sub-basin, western Bonaparte Basin, Australia. *Special Publication - Northern Territory Geological Survey*, 1, 31.

Erdmann, M., (1999) Gas generation from overmature Upper Jurassic source rocks, Northern Viking Graben, pp. 128. Berichte des Forschungszentrum Jülich.

Fujii, T., O'Brien, G.W., Tingate, P.R., Chen, G., (2004) Using 2D and 3D basin modelling to investigate controls on hydrocarbon migration and accumulation in the Vulcan Sub-basin, Timor Sea, Northwestern Australia. *APPEA Journal*, 93-122.

Horsfield, B., Schenk, H.J., Mills, N., Welte, D.H., (1992) An investigation of the in-reservoir conversion of oil to gas; compositional and kinetic findings from closed-system programmed-temperature pyrolysis, *Advances in organic geochemistry 1991; Part 1, Advances and applications in energy and the natural environment*, *19; 1-3*, pp. 191-204. Pergamon, Oxford-New York, International.

IES, (2002) PetroMod© Reference Manual - version 8.0. Jülich, Germany, Jülich, Germany.

Kennard, J.M., Deighton, I., Edwards, D.S., Colwell, J.B., O'Brien, G.W., Boreham, C.J., Anonymous, (1999) Thermal history modelling and transient heat pulses: new insights into hydrocarbon expulsion and "hot flushes" in the Vulcan Sub-Basin, Timor Sea. *APPEA Journal*, 39(1), 177-207.

Kivior, T., Kaldi, J.G., Lang, S.C., (2002) Seal potential in Cretaceous and Late Jurassic rocks of the Vulcan Sub-basin, North West Shelf, Australia. *APPEA Journal*, 42(1), 203-224.

Longley, I.M., Buessenschuett, C., Clydsdale, L., Cubitt, C.J., Davis, R.C., Johnson, M.K., Marshall, N.M., Murray, A.P., Somerville, R., Spry, T.B., Thompson, N.B., (2002) The North West Shelf of Australia; a Woodside perspective. *The Sedimentary Basins of Western Australia: Proceedings of Petroleum Exploration Society of Australia Symposium*, 3, 27-88.

Mango, F.D., (1996) Transition metal catalysis in the generation of natural gas. *Organic Geochemistry*, 24(10-11), 977-984.

Mango, F.D., (1997) The light hydrocarbons in petroleum: a critical review. *Organic Geochemistry*, 26(7-8), 417-440.

Michels, R., Enjelvin-Raoult, N., Elie, M., Mansuy, L., Faure, P., Oudin, J.-L., (2002) Understanding of reservoir gas compositions in a natural case using stepwise semi-open artificial maturation. *Marine and Petroleum Geology*, 19(5), 589-599.

Pedersen, K.S., Fredenslund, A., Thomassen, P., (1989) *Properties of oils and natural gases*. Gulf Publishing Company, Houston.

Schenk, H.J., Horsfield, B., Krooss, B., Schaefer, R.G., Schwochau, K., (1997) Kinetics of petroleum formation and cracking, *Petroleum and basin evolution; insights from petroleum geochemistry, geology and basin modeling*. Springer, Berlin, Federal Republic of Germany.

Yalcin, M.N., Littke, R., Sachsenhofer, R.F., (1997) Thermal history of sedimentary basins, *Petroleum and basin evolution; insights from petroleum geochemistry, geology and basin modeling*, pp. 71-167. Springer, Berlin, Federal Republic of Germany.

Yielding, G., Freeman, B., Needham, D.T., (1997) Quantitative fault seal prediction. *AAPG Bulletin*, 81(6), 897-917.

Appendix 1

Compositional Kinetic Models

Table 14 Activation energies and frequency factors used for each compound of the compositional kinetic models.

G005732 4-Comp_Crack	Methane	C2-C5	PK_C6-C14	PK_C15+
Ratio [%]	6.09	10.98	35.57	47.36
Sorption [g/gKerC]	0.1	0	0	0
Frequency Factor [my^{-1}]	5.1924E+26	5.1924E+26	5.1924E+26	5.1924E+26
Activation Energy		**Initial Ratio**		
44	0.06	0.067	0.073	0.091
45	0.045	0.05	0.055	0.068
46	0.534	0.592	0.652	0.803
47	0.105	0.117	0.129	0.158
48	0	0	0	0
49	0	0	0	0
50	17.605	19.471	22.197	26.53
51	23.035	24.838	27.51	30.732
52	18.953	19.215	18.94	19.719
53	20.069	18.038	15.404	11.081
54	7.275	6.539	5.585	4.017
55	4.553	4.092	3.494	2.514
56	2.853	2.564	2.19	1.575
57	2.219	1.994	1.703	1.225
58	0	0	0	0
59	0.807	0.725	0.619	0.445
60	1.542	1.386	1.183	0.851
61	0	0	0	0
62	0.346	0.311	0.265	0.191
63	0	0	0	0
64	0	0	0	0
Sum	100	100	100	100

G005733 4-Comp_Crack_Plover	Methane	C2-C5	PK_C6-C14	PK_C15+
Ratio [%]	7.96	10.83	33.71	47.51
Sorption [g/gKerC]	0.1	0	0	0
Frequency Factor [my^{-1}]	4.8386E+28	4.8386E+28	4.8386E+28	4.8386E+28
Activation Energy		**Initial Ratio**		
46	0	0	0	0
47	0	0	0	0
48	0	0	0	0
49	0.146	0.207	0.247	0.237
50	0	0	0	0
51	0.254	0.361	0.429	0.413
52	0.127	0.18	0.215	0.206
53	0	0	0	0
54	0	0	0	0
55	10.373	14.747	17.547	16.867
56	7.513	10.398	18.16	15.419
57	9.216	11.564	18.928	16.07
58	7.121	9.049	12.584	10.592
59	7.507	9.308	11.209	8.707
60	4.866	6.033	7.265	5.643
61	11.929	8.606	3.025	5.829
62	7.49	5.403	1.899	3.66
63	7.111	5.13	1.803	3.475
64	4.355	3.142	1.104	2.128
65	4.187	3.02	1.062	2.046
66	1.641	1.184	0.416	0.802
67	4.628	3.339	1.174	2.262
68	0	0	0	0
69	4.081	2.945	1.035	1.994
70	1.473	1.062	0.373	0.72
71	0.505	0.364	0.128	0.247
72	0	0	0	0
73	5.47	3.946	1.387	2.673
Sum	99.99	99.99	99.99	99.99

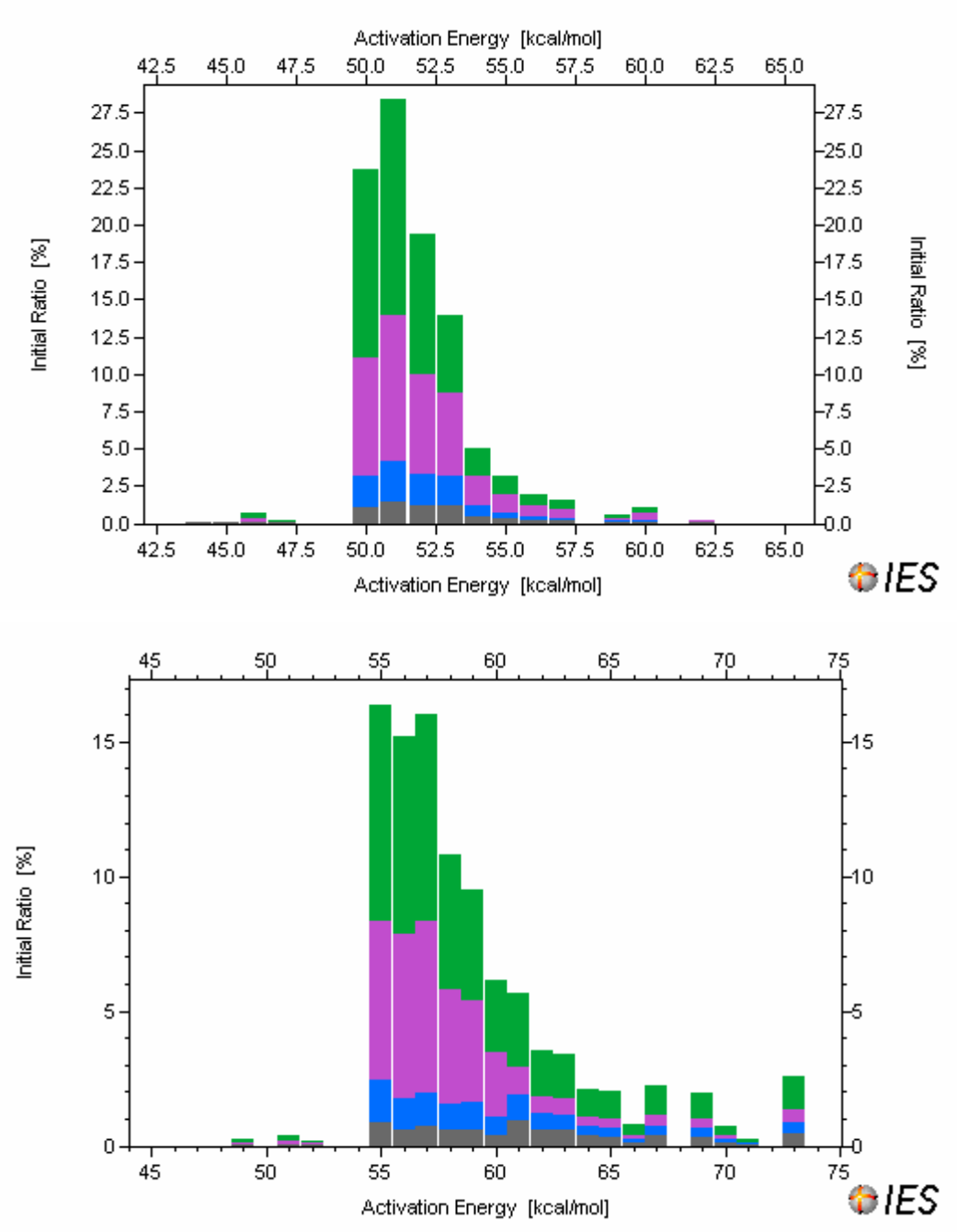

Figure 28 Distribution of activation energies of the source rocks and subdivision of the individual energies into potentials for different compounds. Upper: Compositional kinetic G005732 4-Comp_Crack (Vulcan sequence). Lower: G005733 4-Comp_Crack_Plover for the Plover source rock interval. Grey: Methane, blue: C2-C5, pink: PK C6-C14; green: PK C15+.

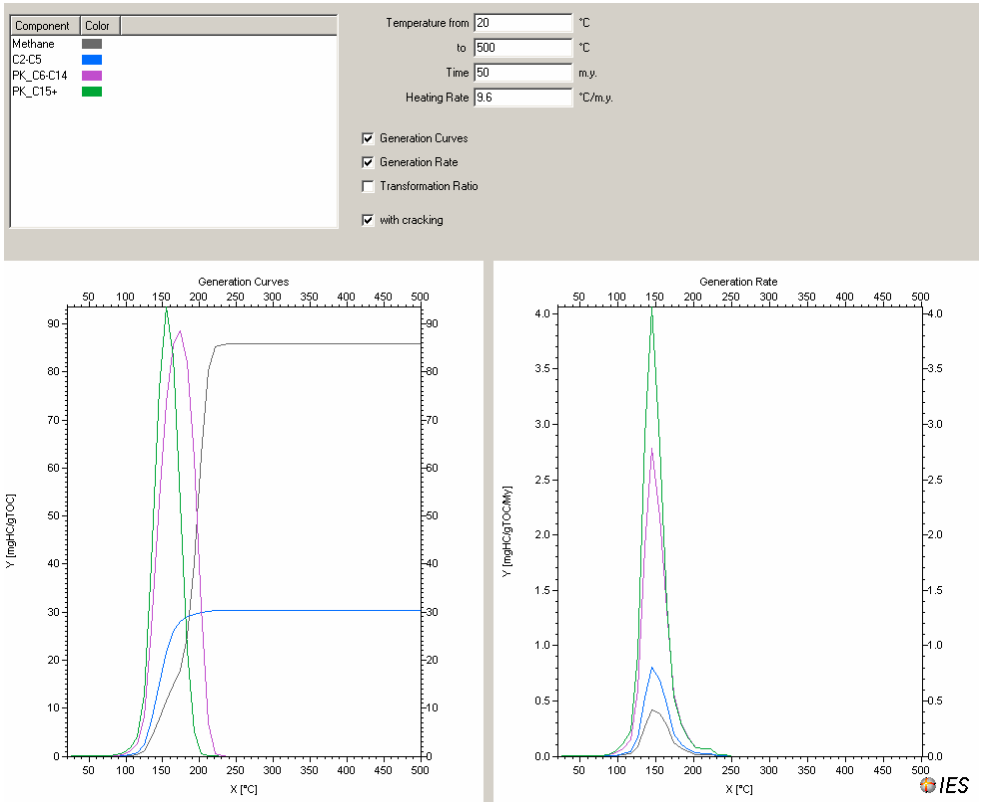

Figure 29 Generation rates and curves Vulcan source rock compositional kinetics.

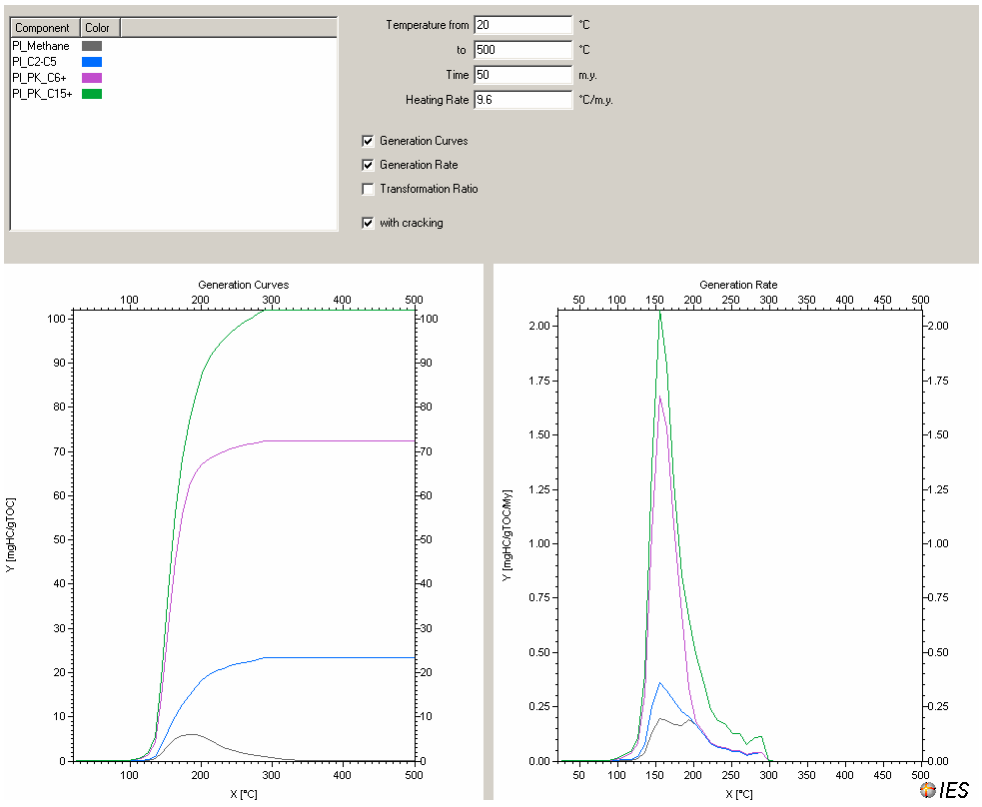

Figure 30 Generation rates and curves for the Plover source rock compositional kinetics.

Cumulative Volumes

Table 15 Cumulative masses (in Mtons) of the petroleum systems calculated for Scenario 1.

Scenario 1	Remaining					Generation	Generated by
Facies	Potential	Accumulated	Liquid	Vapor	Adsorbed	Balance	Primary Cracking
Pliocene	0.0	3.1	3.1	0.0	0.0	0.0	0.0
Mionene	0.0	4.8	4.8	0.0	0.0	0.0	0.0
Eocene	0.0	7.5	7.5	0.0	0.0	0.0	0.0
Paleocene	0.0	6.6	6.6	0.0	0.0	0.0	0.0
U_Creta_SS50%	0.0	6.9	6.9	0.0	0.0	0.0	0.0
U_Creta_SS75%	0.0	0.5	0.5	0.0	0.0	0.0	0.0
U_Cret_(Puffin)	0.0	18.2	18.2	0.0	0.0	0.0	0.0
L_Cretaceous	0.0	39.7	39.6	0.1	0.0	0.0	0.0
U_Vulcan(sq-4c)	0.0	54.7	54.1	0.6	0.0	0.0	0.0
L_Vulcan_U(sq-4b)	0.0	206.7	204.7	2.0	0.0	-10.1	0.0
L._Vulcan_L(sq-4a)_SW	0.0	0.0	0.0	0.0	0.0	0.0	0.0
L._Vulcan_L(sq 4a)_(Montarra)	14601.0	12450.0	8770.7	493.1	3185.9	14649.0	20823.0
Plover_Res	0.0	378.1	356.8	21.3	0.0	-65.6	0.0
Plover_Res	0.0	0.0	0.0	0.0	0.0	0.0	0.0
M_Jura_and_Triassic	0.0	0.0	0.0	0.0	0.0	0.0	0.0
total	14601.0	13176.7	9473.4	517.1	3185.9	14573.3	20823.0

Table 16 Cumulative masses (in Mtons) of the petroleum systems calculated for Scenario 2.

Scenario 2	Remaining					Generation	Generated by
Facies	Potential	Accumulated	Liquid	Vapor	Adsorbed	Balance	Primary Cracking
Pliocene	0.0	3.0	3.0	0.0	0.0	0.0	0.0
Mionene	0.0	4.8	4.8	0.0	0.0	0.0	0.0
Eocene	0.0	7.4	7.4	0.0	0.0	0.0	0.0
Paleocene	0.0	6.5	6.5	0.0	0.0	0.0	0.0
U_Creta_SS50%	0.0	7.7	7.7	0.0	0.0	0.0	0.0
U_Creta_SS75%	0.0	0.7	0.7	0.0	0.0	0.0	0.0
U_Cret_(Puffin)	0.0	18.6	18.6	0.0	0.0	0.0	0.0
L_Cretaceous	0.0	39.9	39.8	0.1	0.0	0.0	0.0
U_Vulcan(sq-4c)	0.0	54.2	53.6	0.6	0.0	0.0	0.0
L_Vulcan_U(sq-4b)	0.0	207.2	205.2	2.0	0.0	-9.9	0.0
L._Vulcan_L(sq-4a)_SW	428.6	179.8	98.9	0.0	80.9	205.8	208.3
L._Vulcan_L(sq 4a)_(Montarra)	14639.0	12429.0	8750.2	494.5	3184.8	14624.0	20786.0
Plover_Res	0.0	398.9	377.7	21.1	0.0	-64.6	0.0
Plover_Res	0.0	0.0	0.0	0.0	0.0	0.0	0.0
M_Jura_and_Triassic	0.0	0.0	0.0	0.0	0.0	0.0	0.0
total	15067.6	13357.8	9574.3	518.4	3265.7	14755.3	20994.3

Table 17 Cumulative masses (in Mtons) of the petroleum systems calculated for Scenario 3.

Scenario 3	Remaining					Generation	Generated by
Facies	Potential	Accumulated	Liquid	Vapor	Adsorbed	Balance	Primary Cracking
Pliocene	0.0	5.4	5.4	0.0	0.0	0.0	0.0
Mionene	0.0	6.6	6.6	0.0	0.0	0.0	0.0
Eocene	0.0	9.4	9.4	0.0	0.0	0.0	0.0
Paleocene	0.0	7.1	7.1	0.0	0.0	0.0	0.0
U_Creta_SS50%	0.0	4.8	4.8	0.0	0.0	0.0	0.0
U_Creta_SS75%	0.0	0.2	0.1	0.1	0.0	0.0	0.0
U_Cret_(Puffin)	0.0	22.5	22.4	0.1	0.0	0.0	0.0
L_Cretaceous	0.0	36.9	35.5	1.4	0.0	0.0	0.0
U_Vulcan(sq-4c)	0.0	40.7	24.9	15.8	0.0	0.0	0.0
L_Vulcan_U(sq-4b)	0.0	210.6	25.8	184.8	0.0	-0.3	0.0
L._Vulcan_L(sq-4a)_SW	431.7	178.3	97.5	0.0	80.8	204.6	205.3
L._Vulcan_L(sq 4a)_(Montarra)	14752.0	14142.0	6717.2	4239.4	3184.9	18138.0	20739.0
Plover_Res	0.0	317.4	287.8	29.6	0.0	-21.9	0.0
Plover_SR	4155.2	401.8	17.4	0.0	384.4	1419.3	1419.3
Plover_Res	0.0	206.0	206.0	0.0	0.0	0.0	0.0
M_Jura_and_Triassic	0.0	0.0	0.0	0.0	0.0	0.0	0.0
total	19338.9	15589.7	7468.0	4471.1	3650.2	19739.8	22363.6

Table 18 Cumulative masses(in Mtons) of the petroleum systems calculated for Scenario 4.

Scenario 4	Remaining					Generation	Generated by
Facies	Potential	Accumulated	Liquid	Vapor	Adsorbed	Balance	Primary Cracking
Pliocene	0.0	5.4	5.4	0.0	0.0	0.0	0.0
Mionene	0.0	6.6	6.5	0.0	0.0	0.0	0.0
Eocene	0.0	9.6	9.6	0.0	0.0	0.0	0.0
Paleocene	0.0	7.6	7.6	0.0	0.0	0.0	0.0
U_Creta_SS50%	0.0	4.7	4.7	0.0	0.0	0.0	0.0
U_Creta_SS75%	0.0	0.2	0.1	0.1	0.0	0.0	0.0
U_Cret_(Puffin)	0.0	22.5	22.4	0.1	0.0	0.0	0.0
L_Cretaceous	0.0	37.8	36.5	1.3	0.0	0.0	0.0
U_Vulcan(sq-4c)	0.0	41.1	25.3	15.8	0.0	0.0	0.0
L_Vulcan_U(sq-4b)	0.0	213.6	25.3	188.3	0.0	-0.3	0.0
L._Vulcan_L(sq-4a)_SW	428.5	180.9	100.0	0.0	80.9	207.6	208.4
L._Vulcan_L(sq 4a)_(Montarra)	14631.0	14029.0	6497.9	4343.3	3187.4	18146.0	20794.0
Plover_Res	0.0	319.0	289.5	29.6	0.0	-20.6	0.0
Plover_SR	4138.3	405.3	17.8	0.0	387.5	1435.0	1435.0
Plover_Res	0.0	202.7	202.7	0.0	0.0	0.0	0.0
M_Jura_and_Triassic	0.0	0.0	0.0	0.0	0.0	0.0	0.0
total	19197.8	15485.8	7251.2	4578.5	3655.8	19767.7	22437.3

Table 19 Cumulative masses(in Mtons) of the petroleum systems calculated for Scenario 5.

Scenario 5	Remaining					Generation	Generated by
Facies	Potential	Accumulated	Liquid	Vapor	Adsorbed	Balance	Primary Cracking
Pliocene	0.0	6.0	6.0	0.0	0.0	0.0	0.0
Mionene	0.0	7.1	7.1	0.0	0.0	0.0	0.0
Eocene	0.0	9.2	9.2	0.0	0.0	0.0	0.0
Paleocene	0.0	5.4	5.4	0.0	0.0	0.0	0.0
U_Creta_SS50%	0.0	12.2	12.1	0.0	0.0	0.0	0.0
U_Creta_SS75%	0.0	2.5	2.5	0.0	0.0	0.0	0.0
U_Cret_(Puffin)	0.0	26.6	26.6	0.0	0.0	0.0	0.0
L_Cretaceous	0.0	40.0	39.4	0.6	0.0	0.0	0.0
U_Vulcan(sq-4c)	0.0	70.4	59.6	10.8	0.0	0.0	0.0
L_Vulcan_U(sq-4b)	0.0	235.1	76.7	158.3	0.0	-0.8	0.0
L._Vulcan_L(sq-4a)_SW	347.9	254.1	174.0	0.0	80.1	295.3	297.7
L._Vulcan_L(sq 4a)_(Montarra)	13398.0	13023.0	6782.4	2913.3	3327.7	19997.0	22529.0
Plover_Res	0.0	687.2	659.8	27.4	0.0	-29.5	0.0
Plover_SR	3937.2	446.0	21.0	0.0	425.0	1592.7	1592.7
Plover_Res	0.0	381.4	381.4	0.0	0.0	0.0	0.0
M_Jura_and_Triassic	0.0	0.0	0.0	0.0	0.0	0.0	0.0
total	17683.1	15206.0	8263.1	3110.5	3832.8	21854.6	24419.4

Appendix 2

Comparison of petroleum physical property predictions of 4-compound and PhaseKinetic models

In the generation of compositional kinetic models using the PhaseKinetic approach the bulk kinetics of the individual samples are populated with compositional data from closed system pyrolysis experiments at increasing levels of transformation (di Primio & Horsfield, 2006). As the initial compositional information is derived from the same experiment in each case a difference with respect to the physical properties of the fluids calculated can only be due to differences in the physical properties of the compound groups or pseudo-components. Figure 31 shows a comparison of 4-compound and 14-compound physical property predictions for one of the standard PetroMod PhaseKinetic models. The results shown are based on implementation of the kinetics in a simple PetroMod 2D model in which a static geologic scenario is heated at a constant geologic heating rate of approximately 1°/Ma. The model used is described in di Primio and Skeie (2004). The evolution of saturation pressure and GOR in Figure 31 indicates that both kinetic models provide essentially very similar predictions, as expected.

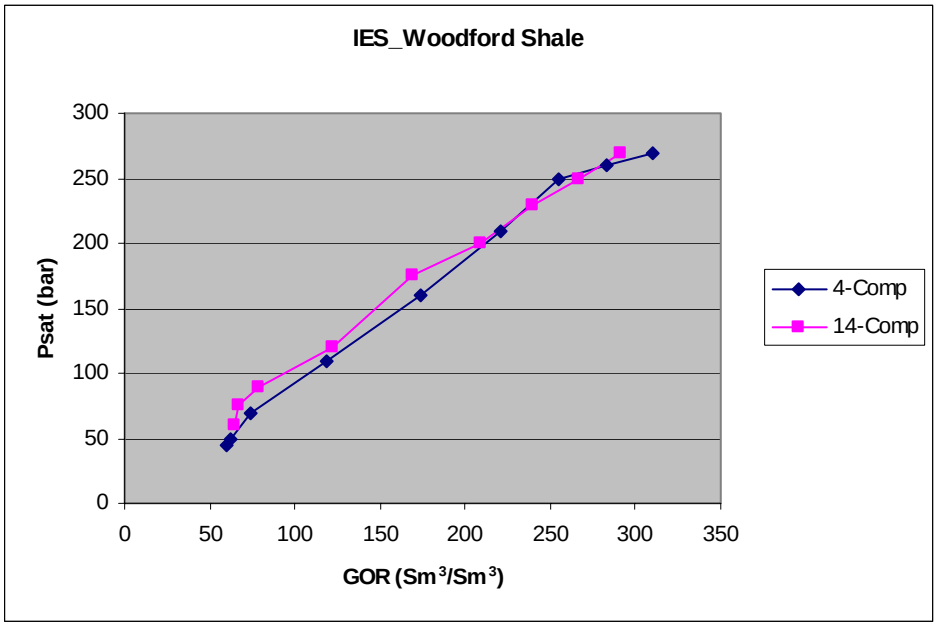

Figure 31 Comparison of 4-compound vs. 14-compound kinetic model predictions for saturation pressure (Psat) and GOR.

The results shown in *Figure 31* are based on the calculations of primary cracking only. In order to take secondary cracking into account the reaction kinetics of cracking, the compounds generated by cracking as well as the proportion of dead carbon remaining need to be defined for each compound which is expected to crack as a function of increasing thermal stress.

In the secondary cracking model implemented in the PhaseKinetics approach, the assumption is made that the entire phase generated by the source rock behaves uniformly with re-

spect to its adsorption potential to dead kerogen. No differentiation is made between a more-adsorptive oil phase and a less adsorptive gas phase as described by Pepper and Corvi (1995). Accordingly the definition of the adsorption potential (0.1 equivalent to 10%) in PetroMod applies to all components and not only the one it is defined for. In the applied model cracking of the adsorbed entire phase (or only those compound for which cracking is defined, i.e. the liquid compounds from C7 onwards) results in the generation of methane by secondary cracking. Due to the change in composition, the volume of the adsorbed phase increases and excess volume is expelled. Methane was selected as the only product of cracking based on observations made on natural petroleum maturity series.

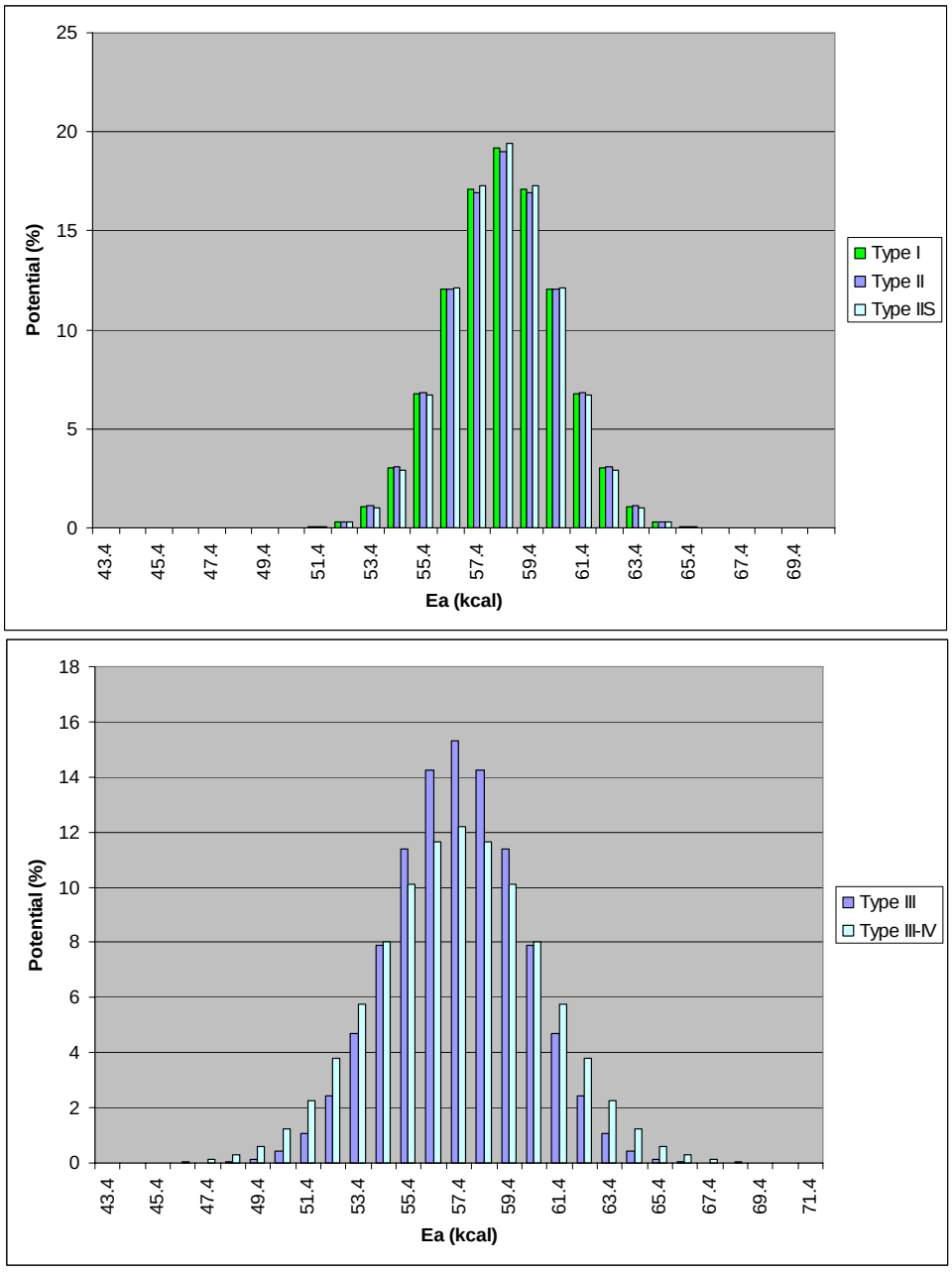

Figure 32 Activation energy distributions for secondary cracking of oil to gas for products different kerogen types after Pepper and Corvi (1995).

Pepper and Corvi (1995) defined secondary cracking kinetics for products of different kerogen types for a two compound system. The main assumption there was that liquid hydrocarbons retained by adsorption to dead carbon within the source rock cracked to gaseous hydrocarbons following the kinetics defined by the parent kerogen type. The activation energy (Ea) distributions for secondary cracking for individual kerogen types are shown in Figure 32. Here it is evident that the Ea distributions are very similar for products from kerogen types I, II and II-S, and for types III and IV. Since all Ea distributions were assigned the same frequency factor differences in kinetics are controlled exclusively by the Ea distribution. For the PhaseKinetic approach the Pepper and Corvi (1995) model had to be expanded to multi component systems. Here the simplification was made that only two Ea distributions are required: one for kerogen types I, II and II-S and a second for the types III and IV. For PhaseKinetics the Type II cracking kinetics of Pepper and Corvi (1995) were subdivided into six sets of kinetics, one for each pseudo-component. In each case a gaussian Ea distribution was assigned to a pseudo-component and each Ea distribution increased by 1 kcal with increasing pseudo-component number. Figure 33 shows the summed cracking kinetics for secondary cracking of the pseudo-components of the 14-compound kinetic models. For the 4-compound kinetics only two liquid pseudo-components are defined. The first is identical to the pseudo-C10 definition of the 14-compound model; the second is equivalent to the sum of the other five pseudo-components. The secondary cracking model was thus simply downscaled from that of the 14-compound model. The cracking kinetics of the 4-compound model are shown in Figure 34.

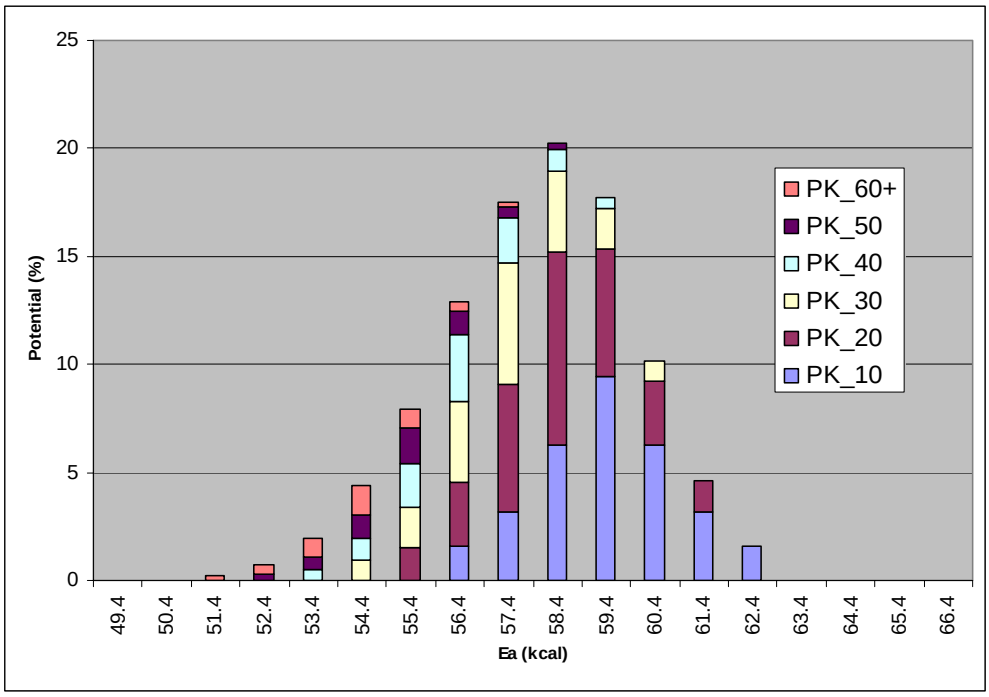

Figure 33 Cracking kinetics implemented in the 14-compound PhaseKinetic models.

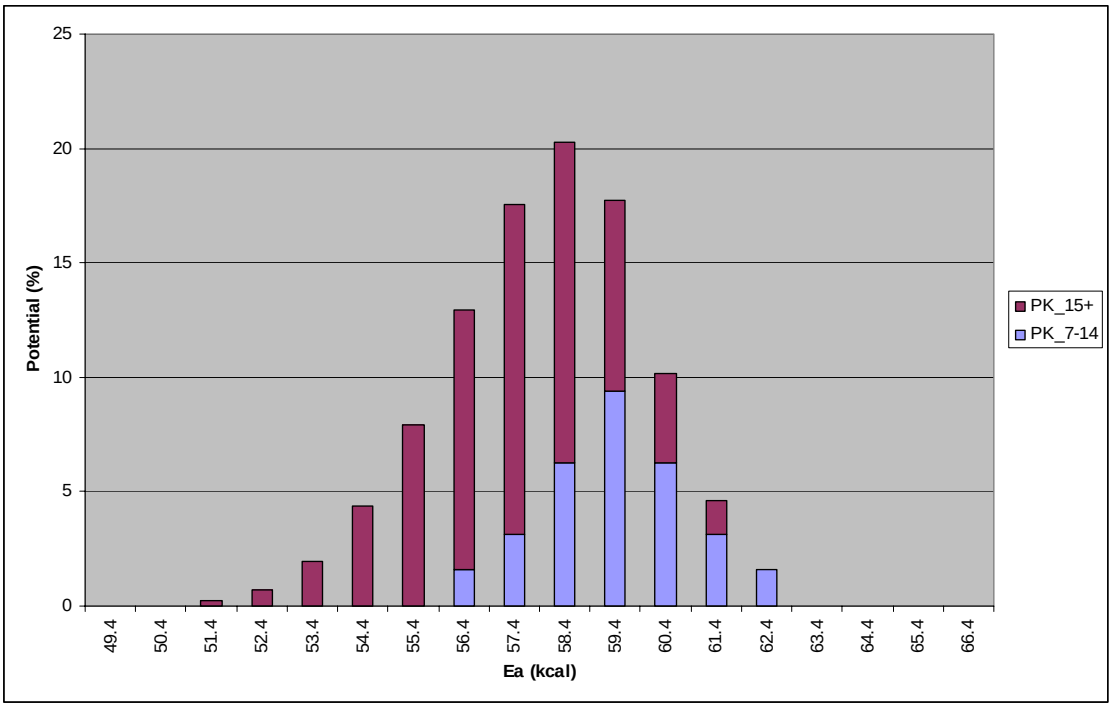

Figure 34 Cracking kinetics implemented in the 4-compound PhaseKinetic models.

As the initial data from which both cracking models were defined is identical the resulting predictions regarding amount and timing of gas generation from secondary cracking is also identical.

Secondary cracking models for Type III and IV kerogen follow the same methodology.

The phase behaviour of migrating petroleum fluids is controlled by the fluids composition. The geological conditions upon which a migrating oil separates into oil and gas are strongly controlled by the gas (C1-C5) composition of the fluid (di Primio et al., 1998). For petroleum phase behaviour gas composition plays the dominant role with respect to the fluids saturation pressure and shrinkage behaviour, however, influence of the liquid fraction composition should not be neglected.

The gross description of oil and gas generation from closed system pyrolysis results, and the surface GORs derived therefrom, are very similar to the GOR distributions observed in nature. Hence, it appears that the relative gas and oil proportions generated as a function of maturity can be estimated based on laboratory experiments.

Compositional predictions are, however, not as straight forward. High methane contents generally result in phase separation at relatively high pressures, i.e. at great depth. A very wet gas composition results in a much lower saturation pressure (Psat) for a given fluid. The sensitivity of gas composition on phase behaviour of migrating hydrocarbons has severe implications for the prediction of petroleum phase behaviour during petroleum generation and migration. Mango (1996; 1997) documented the discrepancy between gas compositions generated by pyrolysis of source rocks or oils and natural fluids. As discussed by Mango (1996; 1997) natural fluids display a much stronger predominance of methane in their gas fractions than observed in source rock pyrolysates. Interestingly, the lack of predictive ability of laboratory experiments is common to all experimental approaches: published gas compositions from closed system hydrous pyrolysis (Andresen et al., 1994), closed system anhydrous pyrolysis (Behar et al., 1991; Dieckmann et al., 1998; Erdmann, 1999; Michels et al., 2002) and open system pyrolysis (Berner et al., 1995) of Type I, II and III source rocks all show the same systematics.

It is commonly known that for genetically related fluids saturation pressure correlates linearly to GOR and formation volume factor (Bo). As discussed above the methane content of a fluid is the most important factor controlling its saturation pressure. Hence, a correction of the gas compositions generated by pyrolysis is possible assuming a linear relationship between the methane proportion of the gas phase (C1-C5) and the fluids GOR. The equation used for methane correction in this study is based on linear regression using a natural dataset from the North Sea representative of the black oil to gas-condensate range (correlation coefficient for the relationship between GOR and C1/C2-5 r2=0.98). The original GOR used as a starting point for the methane correction was that determined on the MSSV pyrolysates and converted to volumetric data by a single stage flash using PVT simulation software.

The characterisation of the generated fluids oil composition (C6+) for phase behaviour assessment is based on the compositional information from MSSV analysis. The resolved compounds from C6 onwards were quantified, their proportions converted to molar amounts and these were summed to a total description of the liquid phase which consisted of a pseudo compound C6 (containing all resolved compounds in the range eluting after Pentane until and including Hexane) and a C7+ fraction (containing the rest of the resolved compounds). The C7+ fraction was further characterised by a molecular weight and density. The molecular weight of the C7+ fraction was determined by subdividing the GC hump (MSSV total mi-

nus resolved compounds) into boiling ranges according to the resolved n-alkanes, and using the average molecular weights of the resolved compounds as representative of the respective hump range. Quantification of the subdivisions led thus to an averaged molecular weight of the entire hump. The density of the C7+ fraction was determined using a C7+ molecular weight – density correlation for natural petroleums from the North Sea.

The compositional description obtained by these methods is ideal for initial phase behaviour calculations. For the determination of a compositional kinetic model, however, a C7+ fraction consisting of molar amount, molecular weight and density was inappropriate. In PVT simulators the C7+ fraction definition is used to calculate a distribution of components representing the total liquid phase. This so called C7+ characterisation consists in representing the hydrocarbons with seven and more carbon atoms as a reasonable number (generally 12) of pseudo-components (with specific equation of state parameters) whereby a logarithmic relationship between the molar concentration zN, of a given fraction and the corresponding carbon number, CN, for CN >7 is assumed (Pedersen et al., 1989). This characterisation leads to the automatic definition of a set of additional compounds of increasing molecular weight (usually up to the molecular weight range corresponding to alkane chainlengths of C80-C100). For this study a series of 6 pseudo compounds were defined: P10, P20, P30, P40, P50 and P60+. The physical properties of the individual pseudo compounds remain constant for all sample types, only their molar proportion varies depending on the samples original composition. This subdivision of the C7+ fraction into 6 additional fractions was tested to be the minimum number of pseudo compounds required for satisfactory calculation of phase behaviour.

The determined PVT descriptions of the fluids at different transformation ratios are used for the definition of the compositional kinetic models. The individual potentials per activation energy derived from the bulk kinetic analysis of the samples are subdivided into 14 subpotentials, one for each compound described in the PVT dataset. The PVT data is assigned to individual bulk potentials based on its transformation ratio. For example bulk potentials below a TR of 20% were assigned the compositional description of the 10% TR MSSV experiment, from 20 to under 40% TR the 30% TR compositional description is used, etc. The final compositional kinetic models, hence, consist of an activation energy distribution for each compound (potentials normalised to 100%) as well as a total potential for each compound (again normalised to 100%). In combination with the sample HI and TOC absolute potentials can be calculated.